Journal of Polymer Research (2025) 32:394
https://doi.org/10.1007/s10965-025-04597-5

ORIGINAL PAPER

Effect of the build orientations on mechanical, superficial and bioactivity properties of additively manufactured PLA and recycled PLA filaments

Şakir Altınsoy[1] · Münife Demirel[2] · Nuray Beköz Üllen[3]

Received: 19 March 2025 / Accepted: 16 September 2025
© The Polymer Society, Taipei 2025

Abstract
This study explores the impact of build orientation on the mechanical, surface, and bioactivity properties of additively manufactured PLA and Re-PLA filaments. PLA and Re-PLA were printed in six orientations at three different filling ratios, with a filament diameter of 1.75 mm, layer thickness of 0.2 mm, and a grid filling shape. The materials were characterized through tensile, flexural, surface roughness, SEM analysis, degradation, and bioactivity (antibacterial and biocompatibility) tests. Results show that build orientation significantly affects the mechanical properties of PLA, with ZXY-ZYX binary groups exhibiting higher bending strength than other orientations. Re-PLA was found to break more uniformly than PLA. No bacterial activity was observed against *S. aureus* or *E. coli* for both materials. Cell viability decreased across all filling ratios in Re-PLA, with a general reduction in cell viability after four days of culture compared to day one. No degradation was detected in PLA and Re-PLA filaments at 20%, 40%, and 60% filling ratios. This study aids in selecting optimal factors like structure orientation and filling ratio for various applications and emphasizes the use of recycled biopolymers from renewable resources, such as PLA, over petroleum-based biodegradable polymers.

Keywords PLA · Recycling · Mechanical properties · Antibacterial and biocompatibility

Introduction

3D printing technology has taken its place as an additive manufacturing (AM) technology that has developed in recent years due to its advantages such as versatile use, simplicity, economy, flexibility in design, suitability for mass production, environmentally friendly green technology orientation, widespread application area, complex and rapid prototyping [1, 2]. AM technology enables high-speed and precision production by extruding a polymer filament layer by layer (x and y-axes) onto a moving plate (z-axis) until a 3D structure is obtained. The fact that there is no need for a mold in advance is a great advantage of the process in terms of time and cost [3]. In particular, the decrease in the prices of polymeric-based AM production machines has shown an increasing growth in personal prototyping manufacturing. Commercially, AM applications lead to industrially important markets such as biomedical, automotive, and aviation prototypes, electronic devices, and electrical home appliances. It is also promising in the medical field, especially in the production of biomedical devices and biomaterials [4–7].

Nowadays, academic research and development studies on sustainable and renewable bioplastics (especially polylactic acid, abbreviated as PLA) have increased in many areas of the industry. PLA, which replaces petroleum-based plastics, is a thermoplastic biopolymer in the aliphatic polyester group. It is produced by fermentation of renewable resources of agricultural waste from corn starch, sugar cane, and sugar beet [8, 9]. In particular, its compostability

✉ Şakir Altınsoy
sakir.altinsoy@yeniyuzyil.edu.tr

1 Department of Biomedical Engineering, Faculty of Engineering and Architecture, Istanbul Yeni Yuzyil University, Istanbul, Turkey

2 Institue of Science and Technology, Istanbul Yeni Yuzyil University, Istanbul, Turkey

3 Department of Metallurgical and Materials Engineering, Faculty of Engineering, Istanbul University-Cerrahpasa, Istanbul, Turkey

Published online: 21 October 2025

makes the product life cycle more usable in terms of sustainability. PLA is the most preferred material in 3D printing technology due to its environmentally friendly green material, biodegradability, and biocompatibility properties [8, 10, 11]. Moreover, considering their sustainable properties, it is possible to improve the properties of 3D printed objects by using new PLA composites in the fields of medicine, tissue engineering, bio-printing, automotive, electrical conductivity, sensor, aerospace, battery, robotics and smart textile industries, packaging, agriculture, and automotive industries [12]. When an error occurs in the production of a product in a 3D printer, the part is considered scrap because it cannot be reused. For these reasons, it creates waste and after each problematic production, faulty parts cause waste of expensive filament material and environmental pollution. It is also important to take into consideration the physiological and biological negative effects of solid wastes in nature. In recent years, demand has increased for renewable resources instead of petroleum-based biodegradable polymers in order to reduce fossil fuel consumption and low greenhouse gas production. PLA makes it possible to recycle the parts that are used and left behind (which can be referred to as waste) and is known as Re-PLA [13–15]. The best waste management during the production phase is the recycling and utilization of waste products back into the raw material chain. Waste filaments can be recycled by various methods and can be reused as raw materials. Thus, both the environment is protected and costs can be minimized. As a filament recycling method, extruders are used and after the filament particles are melted, they are reproduced by flowing through a nozzle of the desired diameter to form a constant thickness value and winding them on spools. During this process, waste can be prevented by recycling the filament as much as needed with the partial production technique from the granular state [16].

In AM technology, parts are manufactured by adding layers on top of each other obtained by melting and stacking the filamentous material by the extruder. AM is a layer-by-layer process and since a crystallographic texture can be present in different build orientations, significantly different mechanical properties can occur. Build Orientation refers to the specific angle and position in which a part is placed on the build platform of a 3D printer during the additive manufacturing process. This orientation can significantly impact the quality, strength, surface finish, and print time of the final part. The choice of build orientation is influenced by factors such as the geometry of the part, the type of 3D printing technology used, and the desired properties of the finished product [17, 18]. Build orientation is known to affect micro and macro-structural properties and associated mechanical properties, but limited information is available on the combined effects of this factor for solid AM parts. Some studies have investigated the effects of multiple parameters on additively manufactured PLA-based structures, but no studies were found that investigated different build orientations [8, 10, 19, 20]. The mechanical behavior of the structures is complex and related to their geometrical properties, but considering the special characteristics of additive-manufactured polymeric-based parts, more academic and industrial knowledge is needed. In this whole process, new standards for solid parts have been created, but more information is needed for specification or standardization studies [21]. However, no studies correlate the different build orientations of additively manufactured PLA and Re-PLA filaments with the mechanical and structural properties. Additive manufacturing enables the production of complex geometries by layer-by-layer construction. The build orientation affects the crystallographic structure, causing mechanical anisotropy, and can create dominant changes in properties. Despite the many advantages of the process, monitoring the effects of structural defects such as residual stress and porosity is necessary to prevent potential problems [22, 23]. The purpose of this study is to examine how build orientations affect mechanical, superficial, and consequently, the bioactivity properties such as the degradation, antibacterial and biocompatibility obtained from tensile and fracture toughness tests of additively manufactured PLA and Re-PLA filaments. The correct choice of parameters will enable designers and manufacturers to achieve good bioactivity and mechanical properties with less variation and uncertainty in parts in terms of manufacturing time and product properties. For this purpose, different tests were carried out, the results obtained were compared and interpreted with the literature and it is aimed that the results will be a resource for those working on the subject and protect nature from waste.

Experimental details

Material

The PLA material used in this study is PLA-PLUS filament of the ELAS-3B brand. PLA-PLUS filament is a material with high impact resistance, strong interlayer adhesion, dimensional stability, low risk of warping, and a matte surface finish. The filament diameter was 1.75 mm, and the layer thickness used in printing was 0.2 mm. It is also suitable for use within a nozzle temperature range of 200–220 °C, a bed temperature of 50–60 °C, and a print speed of 40–60 mm/s. More importantly, since this filament does not contain any special additives or components, it is suitable for continuous recycling and reuse.

Recycling steps

Re-PLA specimens were obtained by recycling the same production material. PLA 3B printing waste was cleaned under industrial conditions at 85 °C using 1% NaOH and 3% active surface solvent. After washing, the materials were vacuum-dried.

Recycled filament production was carried out in a Rondol Microlab twin screw extruder with an L/D ratio of 20 at a rotation speed of 60 rpm.

3D printing process

In this study, a nozzle temperature of 200 °C, a bed temperature of 60 °C, a printing speed of 50 mm/s, and the cooling fan in the "on" mode were used. Specimens were drawn with AutoCAD-2024 and saved as STL extension files. The files were opened in the Ultimaker Cura 5.4.0 program and the necessary supports were made to enable the production of the specimens in the three-dimensional 3D printer. A CREALITY brand CR6SE model printer with a 0.4 mm nozzle diameter was used. The specimens were positioned on the printer table in six different directions. While naming the specimens, a systematic was determined in such a way that the name of the axis parallel to the long edge is the first letter, the name of the axis parallel to the medium-length edge is the second letter, and the name of the axis parallel to the short edge is the last letter. Specimens coded XYZ, YXZ, XZY, YZX, ZXY, and ZYX were produced according to the different build orientations of the specimens on the table. The XYZ, XZY, and ZXY directions were specifically chosen because they represent the basic printing directions in FDM (Fused Deposition Modelling) production. Since the material properties in FDM 3D printing are directionally dependent (anisotropic), the combination of these three orientations allows us to study the mechanical differences between the axis where the layers are formed (Z) and the in-layer axes (X and Y). The Z axis generally shows the weakest strength as it is the interlayer adhesion zone, while the X and Y axes provide higher strength in the interlayer regions where the filaments extend. The XYZ orientation refers to the classical printing direction in which the layers are placed parallel to the printing table, while the XZY and ZXY orientations represent the positioning of the layer structure at different angles. By comparing the behaviour both along the layer and perpendicular to the layer, the effects of production orientation on mechanical performance and surface quality can be more clearly demonstrated, especially for recycled or sterilised materials. Figure 1 (a) and (b) show the dimensions of the specimens and an example of the naming system. A 20% infill rate was used for tensile and three-point bending tests. The specimens used for degradation and bioactivity tests were produced with Ø 25 mm, 3 mm thickness, and (20%, 40%, and 60%) filling ratios. Table 1 shows the production times of tensile, three-point bending, degradation, and bioactivity specimens according to build orientations.

Characterization studies

In this study, production was carried out using PLA and Re-PLA filaments by positioning the table in six different orientation directions, followed by various tests. To this end, tensile tests, three-point bending tests, surface roughness

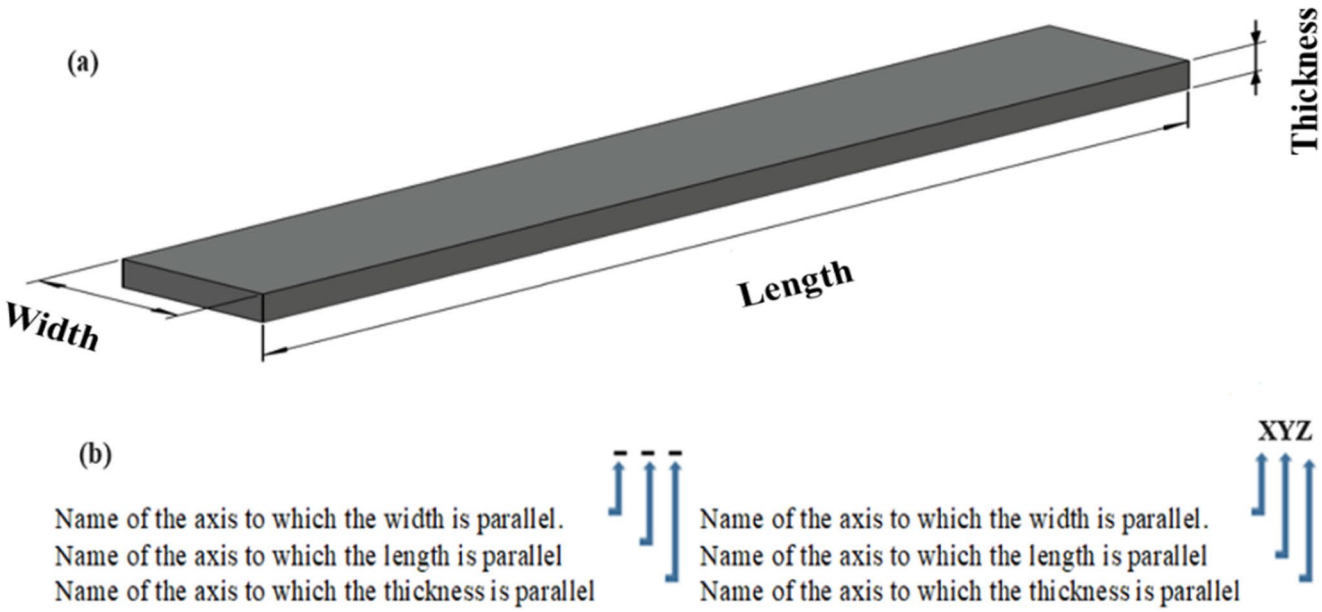

Fig. 1 Dimensions and nomenclature of the test specimens

Table 1 Production times of test specimens according to build orientations

Build orientations	Production times, min		
	Tensile test	Bending test	Bioactivity and degradation test
XYZ	80	49	27
YXZ	80	49	27
XZY	80	57	21
YZX	80	57	21
ZXY	110	72	27
ZYX	110	72	27

measurements, analysis of the fracture mechanisms of broken surfaces, degradation tests, antibacterial tests, and biocompatibility tests were conducted.

Tensile and bending test

In the application of the tensile test, the tensile speed was set to 2 mm/min and the ambient temperature to 25 °C. In the three-point bending test, the distance between the supports was set to 16 mm, the bending speed to 1.3 mm/min, and the ambient temperature to 25 °C. This study was carried out in accordance with EN ISO 14,125 standards. Three measurements were taken for the PLA specimen and three for the Re-PLA specimen in both the tensile and three-point bending tests and the average values were determined. Both tests were performed using an MTS brand 322 test frame model machine. The values in the experimental study were displayed with the help of the "Station Manager" program. Figures 2 (a) and (b) show the drawings of the tensile and three-point bending test specimens used in the experimental study, respectively.

Surface roughness measurements and SEM analysis

Previously tested three-point bending specimens were used in the surface roughness test. Ra (arithmetic mean deviation of the profile) values were measured to determine the surface roughness data of the test specimens. The Ra values of the length, thickness, width, and fractured surfaces of the specimens produced by printing on six different surfaces were measured, respectively. Calculations were performed at three different points for all specimens, and the average value was obtained. For example, the

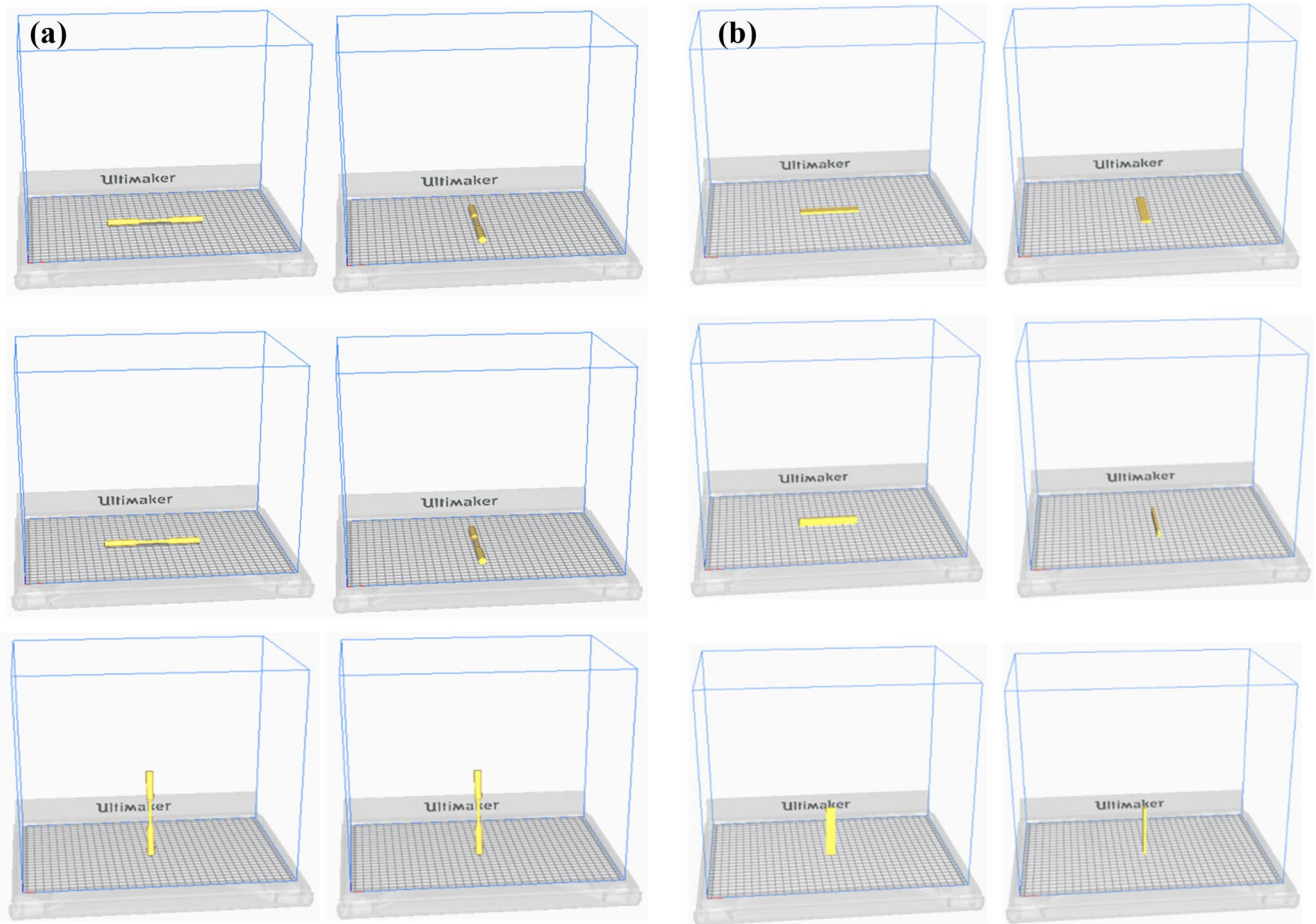

Fig. 2 Drawings of tensile and three-point bending test specimens

length of specimen XYZ was measured from three different points. As a result; twelve measurements were made from specimen XYZ. Surface roughness measurements were carried out with a Mitutoyo brand Surftest SJ-210 model surface roughness device. The results were obtained using the "Surface Roughness Tester SJ-210/310/410" software. Additionally, the fractured surfaces of the PLA and Re-PLA specimens were analyzed using scanning electron microscopy (SEM) to determine the causes of the fractures after testing. SEM imaging was conducted with the Hitachi SU3500 device.

Degradation tests

PLA and Re-PLA specimens were produced with filling ratios of 20%, 40%, and 60%. In the experiments, cylindrical specimens with a diameter of 25 mm and a thickness of 3 mm (Ø25 mm × 3 mm) were used. These specimens were produced using a filament diameter of 1.75 mm, a layer thickness of 0.2 mm, and a grid filling shape. The degradation properties of the PLA and Re-PLA polymers used in the degradation experiments were investigated in PBS buffer. All six specimens for the degradation experiments were placed in 10 ml of PBS buffer in a shaking incubator set to 37 °C and 60 rpm. After 1, 2, 3, 4, 5, 24, 48, 72, 96, 120, 144, and 168 h, 3 ml of sample was taken from each sample and 3 ml of fresh PBS solution was added, leaving a total volume of 10 ml. Spectra were taken in the range of 200–800 nm using a UV spectrophotometer from 3 ml of each sample and the degradation behavior was examined.

Bioactivity test

Since the produced PLA and Re-PLA specimens were considered to be used as biomaterials, antibacterial and cytotoxic tests were performed to analyze their possible effects in the body or during implantation. PLA and Re-PLA specimens produced with filling ratios of 20%, 40%, and 60% were used in these tests. In the experiments, cylindrical specimens with a diameter of 25 mm and a thickness of 3 mm (Ø25 mm × 3 mm) were used. These specimens were produced using a filament diameter of 1.75 mm, a layer thickness of 0.2 mm, and a grid filling shape.

Antibacterial activity tests Antibacterial activity experiments were performed using *E. coli* and *S. aureus* bacteria. The test type performed in this study was zone of inhibition. Mueller-Hinton agar (MHA), which will be used in the studies using *E. coli* and *S. aureus* bacteria was weighed as 38 g, and 1000 mL of distilled water was added to it and homogenized using a magnetic stirrer. After the autoclave process, it was poured into sterile disposable Petri dishes and left to solidify for 1 h. It was then stored at 4 °C.

The other medium used in the studies, Mueller-Hinton broth (MHB), was weighed at 21 g, 1000 mL of pure water was added, and after being homogenized with the help of a magnetic stirrer, it was stored at 4 °C until use. In order to prepare bacterial cultures from bacterial stock cultures, firstly, bacterial suspensions were obtained by incubating a few well-isolated colonies of *E. coli* and *S. aureus* bacteria in MHB at 37 °C and 180 rpm in a shaking incubator for one night. The suspensions were measured in a UV spectrophotometer and prepared to be 10^8 CFU/mL by diluting with MHB until the OD at 600 nm was in the absorbance range of 0.1–0.2. From the prepared bacterial suspension, 100 µL of MHA was added to the Petri dishes, and the bacteria were spread homogeneously on the surface of the Petri dishes with a flame-sterilized glass drigalski. Then, specimens were placed in the Petri dishes and incubated in the incubator at 37 °C for 24 h and the results were observed. 100 µL of the prepared bacterial suspension was added to MHA petri dishes and the bacteria were spread homogeneously on the surface of the Petri dish using a flame-sterilized glass drigalski. Then, the specimens were placed in the Petri dishes and incubated in the incubator at 37 °C for 24 h to observe the results. In the antibacterial activity tests, PLA samples at various filling levels were used as control samples rather than a material with known antibacterial properties. Recycled PLA specimens were compared within their respective filling levels, and PLA and Re-PLA specimens were also compared against each other.

Cytotoxic tests Biocompatibility tests were performed using L929 mouse fibroblast cells using the MTT (3-4.5-dimethylthiazolyl-2.5 diphenyltetrazolium bromide) cytotoxicity test. PLA and Re-PLA specimens with filling ratios of 20%, 40%, and 60% were sterilized in an autoclave, and then 5 mL of FBS-free DMEM F12 medium was placed (10% FBS'Lİ DMEM F12 5mL/45mL DMEM F12) on top and incubated at 37 °C for 7 days. Specimens were taken from the media on days 1, 4, and 7 and stored at +4 °C until use. For the cytotoxicity test, L929 cells were seeded in 25 cm^2 flasks. Cell counts were performed when the cells covered 80% of the flasks. The total cell count was calculated with the following Eq. (1).

$$\begin{aligned} &Total\ Cell\ Count = \ Average\ Cell\ Count \\ &\times Dilution\ Factor\ \times\ 10^4 \\ &= 2 \times\ 50 \times\ 10000 = 1000000\ Cell \end{aligned} \tag{1}$$

According to Eq. 1, cells were seeded with a volume of 100 µL so that there would be 10^4 cells per well. After 24 h of incubation, all of the medium was removed and the cells

were washed with PBS. All of the medium in the specimens on the 1 st, 4th, and 7th days was removed, and 100 µL was added to the wells. For each specimen, 5 replicates were run. Then, the cells were incubated again for 24 h. After 24 h, 10 µL of MTT (Sigma M5655) from the previously prepared stock was added to the wells and incubated in the dark for 3 h. Formazan crystals are formed after incubation, and 100 µL of DMSO (Merck) was added to each well to dissolve them, and then waited for half an hour. Finally, the plate was read at a wavelength of 540 nm on a plate reader device (Thermo Scientific MultiScan). Viability was calculated from the absorbance values obtained. The viability of the cells was calculated according to the equation given in Eq. 2.

$$\%\,Viability = \frac{Experimental\ Group\ Absorbance}{Control\ Group\ Absorbance} \times 100 \qquad (2)$$

Results and discussion

Tensile test results

AM productions of polymeric parts have attracted much attention recently due to its high design flexibility and ability to create complex parts. While a wide variety of parts can be easily manufactured using 3D printers layer by layer according to traditional methods, the printing parameters significantly affect the mechanical properties of the products. It is known that the mechanical properties of parts produced by AM are directly related to the processing parameters. Therefore, optimizing the processing parameters offers a good solution to improve the mechanical properties of specimens produced by the AM production method [24, 25]. Stress-strain graphs of additively manufactured PLA and Re-PLA filaments in different orientations are shown in Fig. 3. A comparison of tensile strength results obtained from graphs of PLA and Re-PLA filaments in different orientations is shown in Fig. 4.

When the stress-strain curves obtained as a result of the tensile tests are examined, it is first seen that the material changes shape at a certain rate in response to the increasing stress. This region is the first region and the shape change that occurs is elastic, that is, it is reversible, or in other words, the cellular structure can return to its former state when the applied stress is withdrawn. In this region, the unit shape change that occurs in response to the applied stress changes linearly and the elasticity modulus is constant. Some cells in the cellular structure may break at the end of the first region. The highest stress value in the second region shows the maximum tensile strength [26].

There is no reversal of the shape change that occurs in this region, that is, plastic shape change has occurred. During the plastic compression that occurs in this region, the area under the stress-strain curve shows the energy storage ability of the structure. This explains the high energy absorption feature of cellular materials. After this region, rupture occurs. When Fig. 3 is examined, it is revealed that

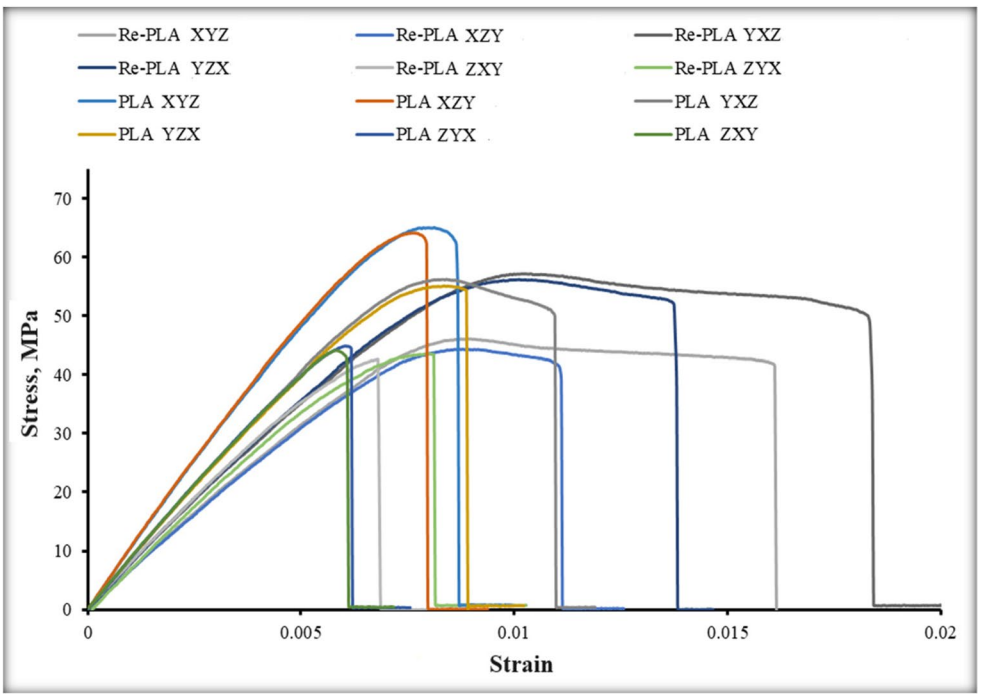

Fig. 3 Stress - strain graph of PLA and Re-PLA filaments in different orientations

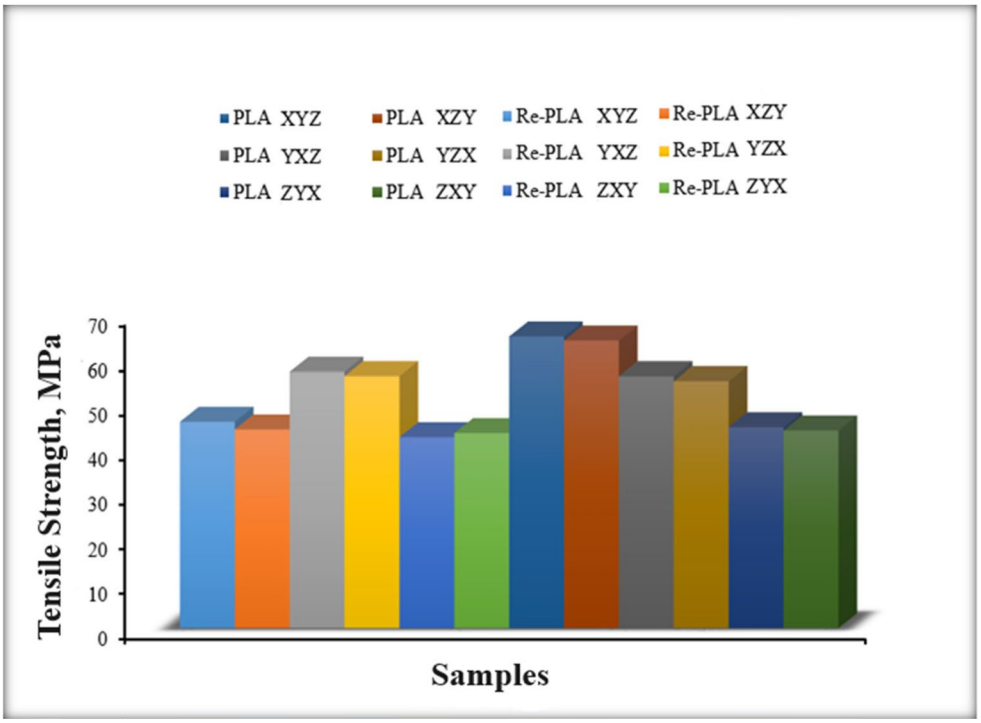

Fig. 4 Comparison of tensile strength results of PLA and Re-PLA filaments in different orientations

the PLA and Re-PLA filaments, which are separated into XYZ-XZY, YZX-YXZ, and ZYX-ZXY binary groups, have almost similar characteristics. The main reason for these differences is the 90° rotation of the specimens while positioning them on the table. Due to these rotations, some voids are formed in the internal structure of the specimens. It has been reported that their strength changes due to these voids [27, 28].

As seen in Fig. 3, it was determined that there was a decrease in stress but an increase in strain values in Re-PLA compared to PLA. The lowest and highest strain values in PLA materials were 0.006 mm/mm and 0.011 mm/mm, respectively, while the lowest and highest strain values in Re-PLA filament were 0.007 mm/mm and 0.019 mm/mm, respectively. This difference is attributed to the change in hardness values after recycling. During the recycling process of Re-PLA filament, several degradations occur in its properties. During the recycling process and production of the filament, extrusion interruptions can create an irregularity that may occur. In addition, microscopic impurities may occur if no filter is used before the filament is extruded [29, 30]. The stress-strain results obtained in this study were found to be consistent with the literature. In order to better interpret the results shown in Fig. 4 and to compare the specimens in their own planes, the differences in the increase and decrease in tensile strength are shown in Table 2.

When the difference between the specimens made of PLA and Re-PLA in the same plane was examined, a decrease in the strength of XYZ and XZY specimens was observed; it was observed that the specimens produced in other planes showed almost similar properties. It was observed that the specimens produced with PLA were more brittle and the specimens produced with Re-PLA were more ductile. It was observed that the specimens produced in YZX and YXZ planes had similar properties in terms of both ductility and maximum tensile strength. The events in question are such that may occur during the synthesis of specimens from the filament. Accordingly, it shows the change in the mechanical properties of the specimens and the properties shown in the experimental tests [28, 29].

The tests were carried out until the specimens broke, the ductility of the polymers did not cause the specimens not to break. As a result of the data obtained, the specimens produced with unmodified PLA material and Re-PLA produced specimens show similar mechanical properties [25]. It is also revealed as a result of the literature research that the decrease in mechanical properties when recycled filaments

Table 2 Changes in tensile strengths of different build orientations

Build orientations	Tensile strength, MPa		Change, %
	PLA	Re-PLA	
XYZ	65.08	46.10	−18.98
XZY	64.17	44.37	−19.80
YXZ	56.24	57.21	+0.97
YZX	55.12	56.24	+1.12
ZYX	44.88	43.56	−1.32
ZXY	44.14	42.64	−1.50

are used is directly related to the lower molecular weight compared to others, which causes recycling [25]. In lattice structures, the arrangement of production directions and loading directions is very effective on mechanical properties [31, 32]. The most important reason why the direction of construction affects the mechanical properties in truss structures produced by the additive manufacturing method is that the amount of pores resulting from the production is different in different construction directions. Delroisse et al. stated that the parts designed and manufactured vertically have fewer pores than the oblique ones, and that two different regions are formed in the obliquely manufactured parts: the upper region with harder, less porous, fine microstructure and the lower region with less hardness, more porous and coarse microstructure [33]. Hanon et al., investigated the effect of 3D printing parameters on the mechanical performance of PLA polymer and its relationship with hardness [34]. The productions were carried out by changing the parameters such as manufacturing direction, indentation angle, and layer height. According to the results of the research, the Young modulus, ultimate tensile strength, and hardness were obtained in the highest edge/perpendicular direction production. The study shows that hardness and tensile strength are directly proportional when the printing direction is variable. Mayén et al., focused on developing a methodology to evaluate the hardness, fatigue, and crack propagation performance of 3D printed plastic parts made of PLA using AM technology [35]. The specimens were produced in different geometries and subjected to various degrees of processing. The research showed that the indentation angle is a leading factor in determining the bulk properties of 3D printed PLA parts.

Bending test results

Flexural elasticity, also called flexural modulus, is the stress-strain ratio at the elastic limit. The maximum bending stress in a bending test is called flexural strength [36]. Three-point bending graph of PLA and Re-PLA filaments in different orientations is shown in Fig. 5. A comparison of flexural strength results of PLA and Re-PLA filaments in different orientations obtained from bending graphs is shown in Fig. 6.

The slope of this linear line obtained gives the bending rigidity of the structure. The highest force value reached on the bending curve is the maximum bending force. The amount of deformation of the structure at the moment of rupture can be defined as the rupture elongation [37]. As a result of the tests performed, it is observed that the bending properties of PLA and Re-PLA filaments vary depending on different orientations. One of the important bending properties on the bending curve is the bending rigidity. The slope of the curve in the elastic region defines the bending rigidity of the specimens. The maximum bending force, which is the bending property, shows the maximum force that the specimens can withstand. When the results of the flexure test experiment given in Fig. 5 are evaluated; it is revealed that the specimens formed from PLA and Re-PLA materials have almost similar characteristics, divided into XYZ-YXZ, XZY-YXZ, and ZXY-ZYX binary groups. It was observed that the groups of specimens separated into binary groups mentioned here were rotated 90° on the table surface [38]. When the binary groups of the specimens formed from PLA and Re-PLA were examined, an increase in the strength of the specimens was generally observed; the specimens

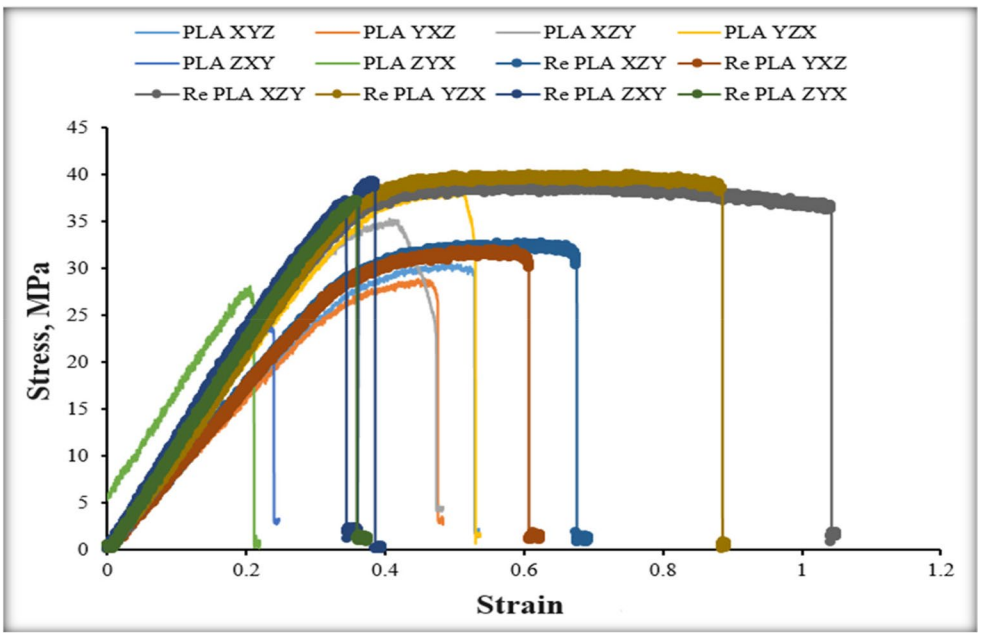

Fig. 5 Three-point bending graph of PLA and Re-PLA filaments in different orientations

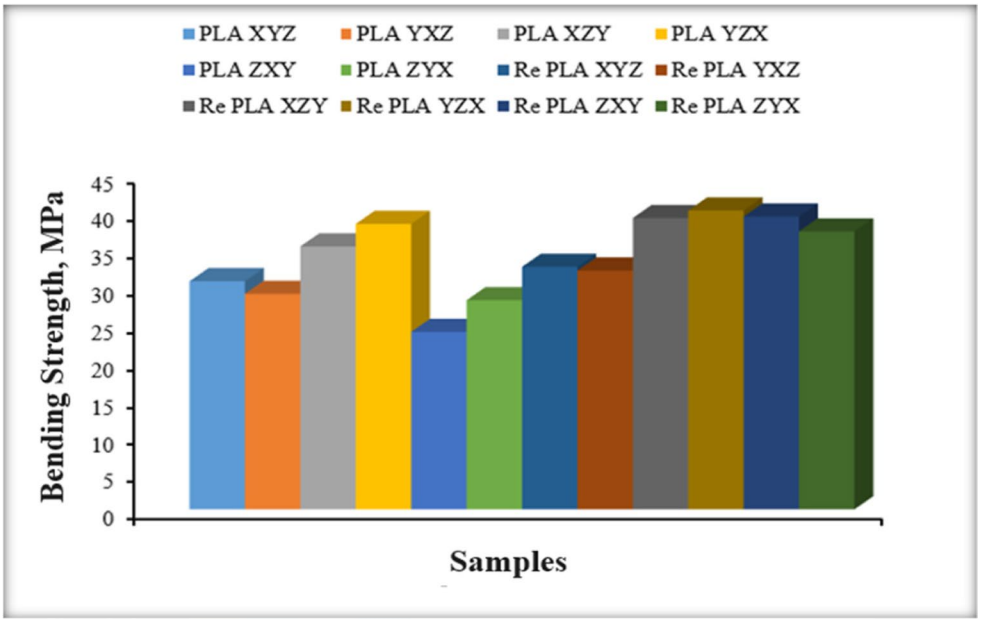

Fig. 6 Comparison of Flexural strength results of PLA and Re-PLA filaments in different orientations

produced in the ZXY-ZYX binary groups showed a higher increase compared to the other binary groups. As seen in the same figure, the bending strength of the specimens produced with Re-PLA is higher than the other specimens. The highest strain value was also obtained in the specimens produced with Re-PLA. Although the flexural strength of PLA specimens is not a significant result, it is small in comparison [38, 39]. It is thought that the high or low flexural strength of the produced specimens depends on the energy flow during production and the difference in surface roughness [31, 40].

In order to better interpret the results shown in Fig. 6 and to compare the specimens in their own planes, the differences in the increase and decrease in flexural strength are shown in Table 3.

It was observed that the specimens produced with PLA were more brittle and the specimens produced with Re-PLA were more ductile. Both PLA and Re-PLA specimens of the XYZ-YZX binary group were similar in terms of ductility and maximum flexural strength. The highest increase was obtained in the ZXY-ZYX binary group. Improving the impact strength of PLA compared to other contemporary filaments used in filament synthesis will enable a wide range of applications by replacing commercial polymers [13]. In the study conducted by Alsalla et al., it was stated that the tensile strength and yield strength were 60% higher in the vertical direction than in the horizontal direction, and the elongation was 40% higher [41].

Table 3 Changes in flexural strengths of different build orientations

Build orientations	Flexural strength, MPa		Change, %
	PLA	Re-PLA	
XYZ	30.62	32.55	−1.93
YXZ	28.92	32.04	+3.12
XZY	35.29	39.10	+3.81
YZX	38.31	40.12	+1.81
ZXY	23.82	39.30	+15.48
ZYX	28.06	37.31	+9.25

Surface roughness results

The important reason for the change in surface quality is the stair step effect that occurs depending on the heat and extrusion time of each layer in additive manufacturing. After the support structures are produced, the thin layer placed on it starts to cool down and shrinks until the next layer is laid, and this affects the next layer and causes the formation of inclined or sagging surfaces [42]. These surfaces prevent the next layer from coming together properly and change the surface structure up to the top layer of the part to be produced. This failure of the layers to come together properly negatively affects the surface roughness at the top level of the produced part. Surface roughness affects dimensional accuracy, production costs, and mechanical performance of parts. Due to this, the development and research carried out to create a good result of surface roughness have paved the way for optimizing production methods. For these reasons, it is important to make surface roughness measurements, which affect the surface quality, the most [43]. A comparison of average Ra values of PLA filaments in different orientations is shown in Fig. 7.

When examining the surface roughness results in the length direction of these specimens produced in different orientations, as shown in Fig. 7; it is noteworthy that the specimen produced in the ZXY orientation exhibits the

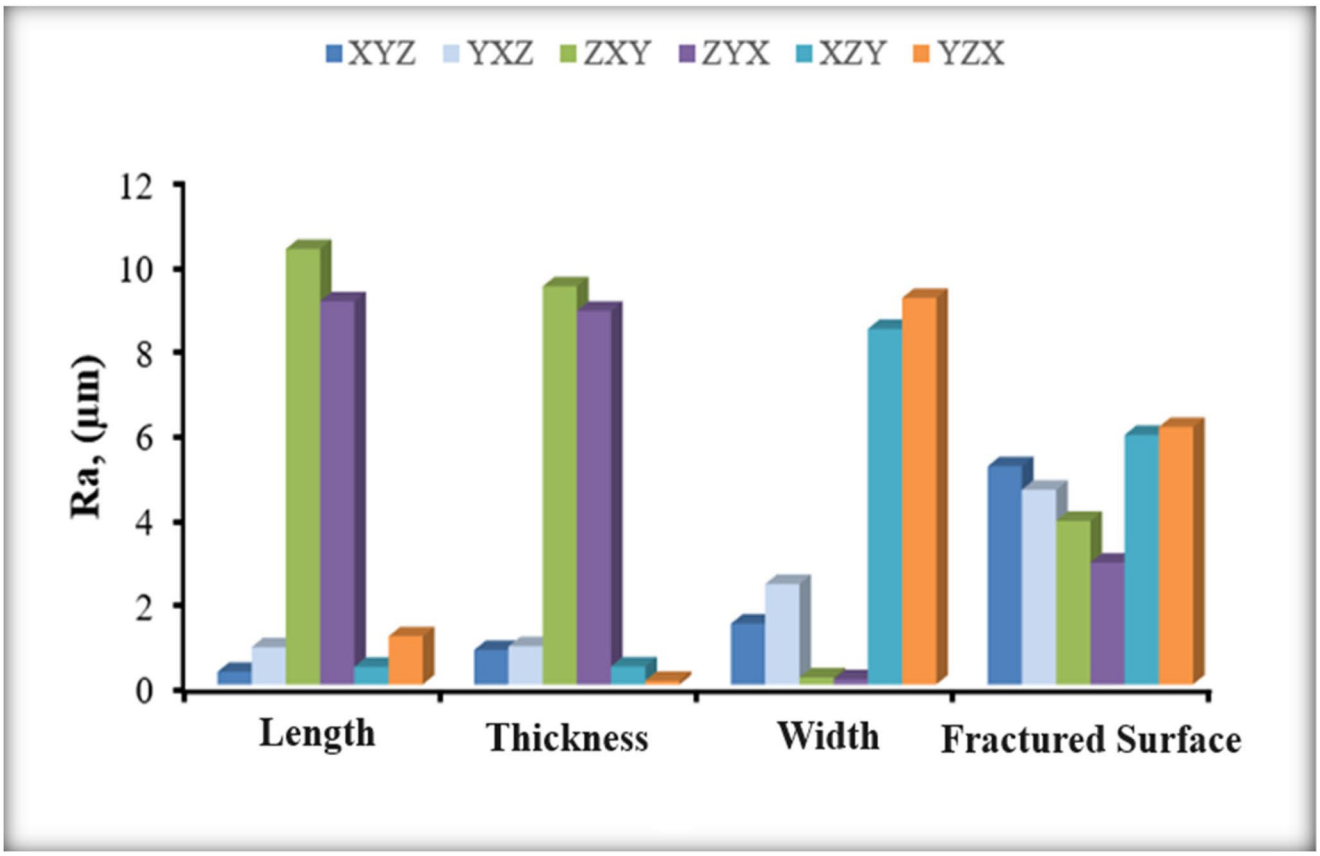

Fig. 7 Comparison of average Ra values of PLA filaments in different orientations

highest surface roughness, while the specimen produced in the XYZ orientation shows the lowest surface roughness. The main reason why the ZXY and ZYX orientations consistently exhibit the highest Ra values is the orientation of the layers. In these orientations, layers are stacked perpendicular to the surface where the surface roughness measurement is made during production. This causes each layer line to be visible on the surface. The interlayer boundaries and transition zones create greater surface irregularity, leading to an increase in the Ra value. Therefore, this high surface roughness is directly related to the distinct perception and visibility of layer lines on the measured surface. In terms of surface roughness measured along the length direction, Ra values showed significant variation depending on the printing orientation. Compared to the XYZ specimen, Ra increased in XZY (40%), YXZ (195%), YZX (281%), ZXY (3349%), and ZYX (2934%). The Ra values for the XYZ, XZY, YXZ, and YZX specimens remained within the 0–1.5 µm range, while much higher values between 9 and 10.5 µm were observed for the ZXY and ZYX specimens. When examining the thickness direction, the ZXY specimen again exhibited the highest surface roughness, while the YZX specimen had the lowest. Compared to XYZ, Ra increased by 10%, 1053%, and 982% in YXZ, ZXY, and ZYX, respectively, but decreased by 48% and 90% in XZY and YZX specimens. Similar to the length direction, Ra values for XYZ, XZY, YXZ, and YZX remained within 0–1 µm, while ZXY and ZYX again showed substantially higher roughness in the 8–9.5 µm range. Looking at the width direction, the surface texture varied significantly. The YZX specimen displayed the highest roughness, whereas ZYX had the lowest. Ra increased by 487%, 65%, and 535% in XZY, YXZ, and YZX, respectively, and decreased by 88% and 91% in ZXY and ZYX. The Ra values were measured between 1 and 2.5 µm for XYZ and YXZ, 8–9.5 µm for XZY and YZX, and only 0–0.5 µm for ZXY and ZYX. Finally, on the fracture surfaces, a similar trend was observed. The YZX specimen again showed the highest roughness, while ZYX had the lowest. Compared to the XYZ orientation, Ra increased slightly in XZY (14%) and YZX (18%) and decreased in YXZ (10%), ZXY (25%), and ZYX (44%). Here, Ra values ranged between 4 and 5 µm for XYZ and YXZ, 5–6 µm for XZY and YZX, and 2–4 µm for ZXY and ZYX.

Changing the production direction is also effective in giving the necessary time for the melted and laid filament to cool. Laying another layer before the laid layer has cooled sufficiently can increase the temperature in the part and

cause thermal stress. In addition, having a higher heat transfer surface area compared to the production direction causes the surface quality to increase. In the literature studies on this subject, it has been stated that thermal diffusion creates a stress effect on part [44]. In this study, when the PLA specimens printed in the same way in different orientations were examined, it was observed that the surface roughness was higher on the surfaces printed on the Z-axis when we looked at the length and thickness. Unlike the other surfaces, it was observed that the average roughness decreased on the surfaces printed on the Z-axis in the measurements made at the width and broken surface points. The characteristic changes in the surface roughness of the specimens are due to the different positioning on the table due to the constant production methods [45–47]. A comparison of average Ra values of Re-PLA filaments in different orientations is presented in Fig. 8.

Figure 8 shows how the surface roughness of the specimens varies depending on the build orientation and measurement direction. Along the length direction, the highest Ra value was recorded in the ZXY specimen, while the lowest was seen in the YZX orientation. Compared to the XYZ reference, Ra increased significantly in the XZY (57%), ZXY (2310%), and ZYX (2264%) specimens, whereas it decreased in the YXZ (56%) and YZX (90%) orientations. In this direction, Ra values ranged between 0 and 1 µm for XYZ, XZY, YXZ, and YZX specimens, while much higher values (12–13 µm) were measured for the ZXY and ZYX orientations. When considering the thickness direction, the ZYX specimen again showed the highest surface roughness, while XZY had the lowest. In comparison to the XYZ specimen, YXZ, YZX, ZXY, and ZYX all exhibited increases in Ra values by 240%, 70%, 2950%, and 3185%, respectively. The XZY specimen, on the other hand, showed a 30% decrease. The Ra values remained within 0–1 µm for XYZ, XZY, YXZ, and YZX, but ranged between 2 and 10 µm for ZXY and ZYX. Surface roughness measurements along the width direction revealed a different trend. Here, XZY had the highest Ra value, while ZXY showed the lowest. Compared to XYZ, there was a slight increase (9%) in the XZY specimen, but noticeable decreases in YXZ (62%), YZX (60%), ZXY (88%), and ZYX (63%). The Ra values for XYZ and YXZ were around 8–9 µm, while YXZ, YZX, and ZYX ranged between 3 and 3.5 µm. The Ra value for ZXY was the lowest, measured at approximately 1.013 µm. The observation of low surface roughness values in the thickness direction and high surface roughness values in the width direction in the specimens produced in XZY orientation

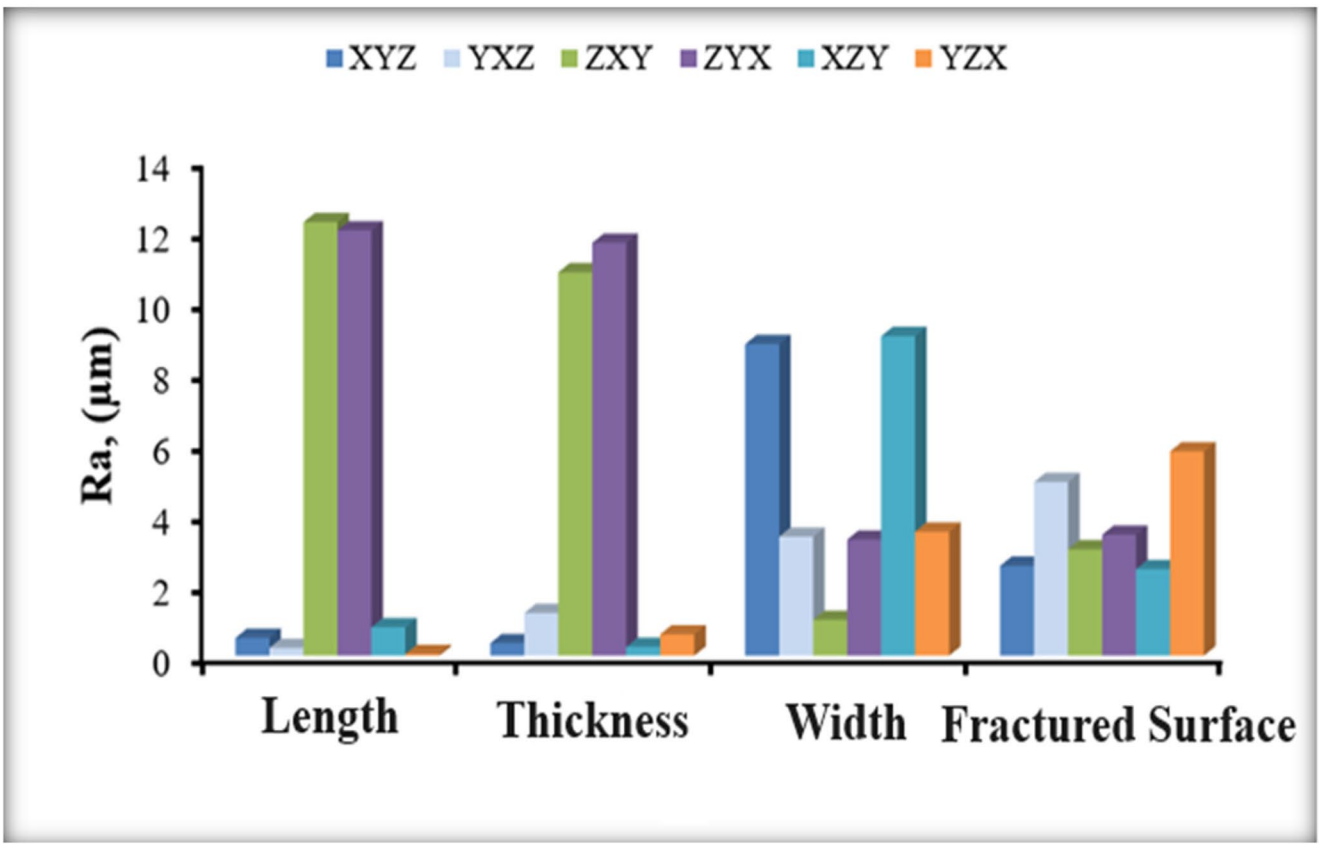

Fig. 8 Comparison of average Ra values of Re-PLA filaments in different orientations

is directly related to the anisotropic cooling behaviour and nozzle movement patterns in the printing process. In this orientation, since the filaments are laid on top of each other in layers, the changing directional movements of the nozzle, especially along the width, leave more pronounced marks on the surface, which increases the roughness values. On the other hand, since the layer transitions in the thickness direction are smoother, the roughness remains at a low level. In addition, stress differences due to cooling rates in different axes can cause microscopic distortions on the surface of the material. This leads to surface characteristics related to interlayer adhesion and material flow direction becoming more pronounced, especially in angled orientations such as XZY. Therefore, the XZY orientation clearly reflects the effects of both anisotropic mechanical behaviour and printing parameters on the surface morphology [48–50]. Finally, on the fracture surfaces, the highest surface roughness was again observed in the YZX specimen, while XZY had the lowest. According to the figure, Ra values increased by 93% in YXZ, 119% in YZX, 18% in ZXY, and 34% in ZYX, relative to XYZ. A slight decrease of 4% was noted in the XYZ specimen. Ra values for XYZ, XZY, ZXY, and ZYX were measured between 2 and 3.5 µm, whereas higher values, between 5 and 6 µm, were seen in the YXZ and YZX specimens. These results clearly show that surface roughness is strongly influenced by the orientation in which the part is printed. The differences are largely due to variations in pore distribution that occur depending on how the material is deposited during the additive manufacturing process [51].

According to average Ra values, column graphs were made in order to make a comparative interpretation of additively manufactured PLA and Re-PLA filaments. Figure 9 (a), (b), and (c) show the comparison of the average surface roughness results of PLA and Re-PLA filaments, for XYZ-YXZ, XZY-YZX, and ZXY-ZYX axes, respectively.

When the results shown in Fig. 9 are investigated; it is seen that the characteristics of the XYZ-YXZ, XZY-YZX, and ZXY-ZYX binary groups in terms of Ra surface roughness in both PLA and Re-PLA are equal. While materials with low surface roughness values show better mechanical properties; they show lower mechanical properties than materials with higher surface roughness [47, 52]. The results obtained in this section are in agreement with the results of tensile and three-point bending tests. The results demonstrate a direct relationship between surface roughness and mechanical properties. The higher Ra values observed, particularly in specimens produced along the Z-axis, indicate reduced tensile and flexural strength due to the presence of more voids and weak interlayer adhesion in these orientations. In contrast, lower Ra values were achieved in XYZ and similar orientations due to the smoother surface structure, resulting in improved mechanical performance. Surface defects occurring in certain orientations, such as incomplete interlayer adhesion, void formation, or microstructural irregularities, cause stress to concentrate in specific areas under loading, thereby increasing adverse effects such as fracture or deformation. Especially under loads applied perpendicular to the Z-axis, the mechanical strength of the structure is significantly reduced due to these interlayer weaknesses.

It has been observed that the production direction in additive manufacturing is a component of part production, and accordingly, it can affect its weight, surface quality, and geometric accuracy. It has been observed that the production direction affects the cooling time of the current layer until the next layer is laid, and thus affects the shrinkage of the PLA material, thus affecting the surface quality. As a result, in additive manufacturing, the production of the part with balanced layers in the production direction affects the mechanical properties and surface quality of the part [53].

SEM analysis

The mechanical properties of specimens are maximally related to their microstructural properties and their microstructure can be modified by the applied parameters. Therefore, in order to better understand the mechanical properties of materials, their structures should be examined in detail [54]. Based on these explanations, SEM image analysis of the fractured surfaces was performed. Figures 10, 11 and 12 show the SEM images at different magnifications of PLA filament with respect to XYZ, XZY, and ZXY axes, respectively. In Figs. 13, 14 and 15; SEM images at different magnifications of Re-PLA filament according to XYZ, XZY, and ZXY axes, respectively.

When the fracture patterns in the SEM images were examined in general, it was seen that some ductile deformation occurred due to the cellular structure. When examining the SEM images of PLA produced along different axes, as shown in Figs. 10 and 11, and 12, the rough surfaces observed on the fracture surface indicate plastic deformation. Micro-cracks were observed on the fracture surfaces. The flat appearance of the fracture surface in Fig. 10 indicates brittle fracture. Figure 11 shows a two-phase (semi-crystalline) structure consisting of crystalline and amorphous regions on the fracture surface. Figure 12 shows a two-phase structure consisting of a dispersed phase and a matrix phase.

Looking at the filament cross-section SEM analysis images, it is seen that Re-PLA contains more rough regions and cracks than PLA as shown in Figs. 13 and 14, and 15. These regions negatively affect the mechanical behavior of the specimens produced during the tests. The surface roughness value in the specimens is inversely proportional to

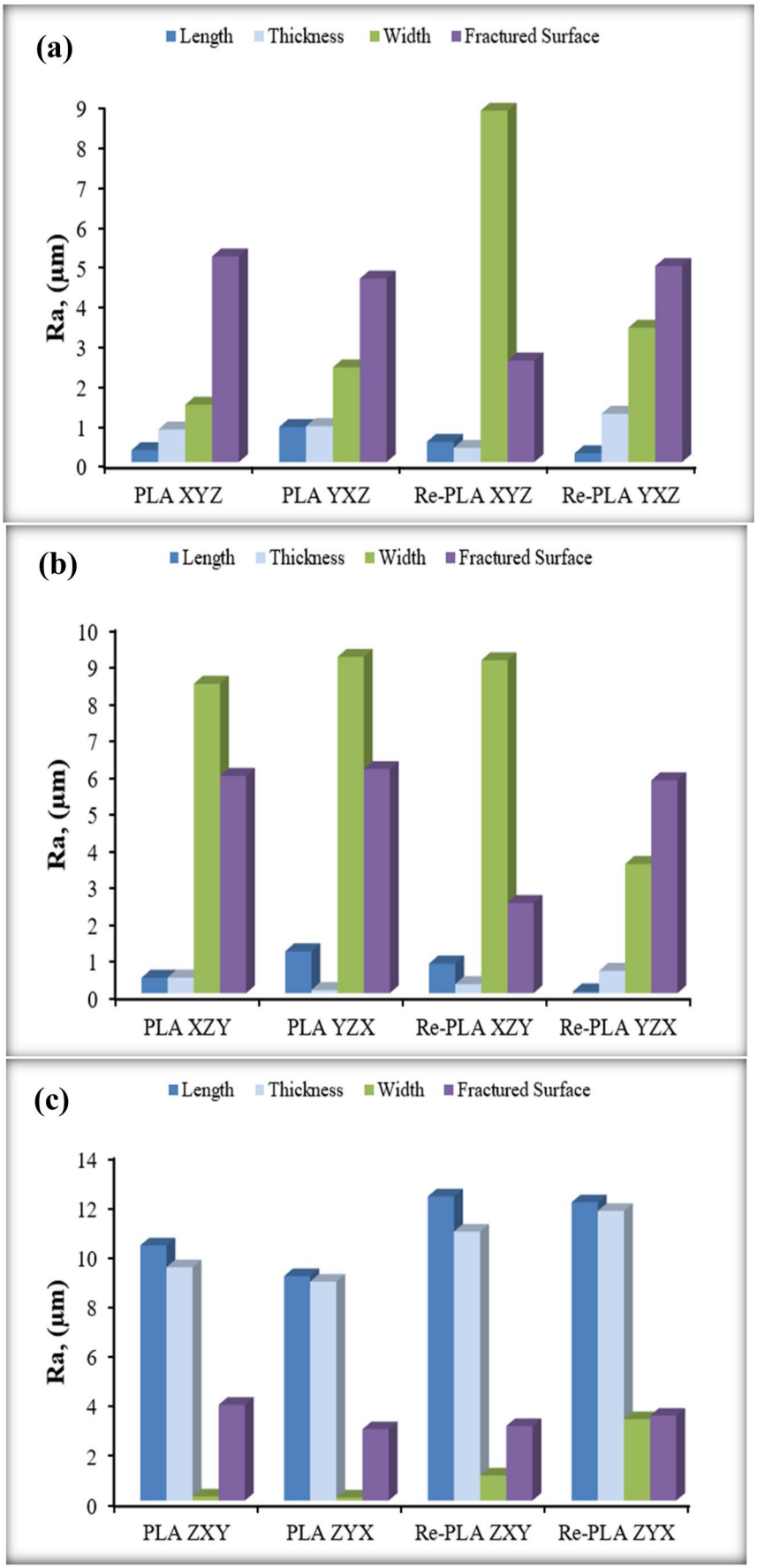

Fig. 9 Comparison of average Ra values of PLA and Re-PLA filament for (**a**) XYZ-YXZ, (**b**) XZY-YZX, and (**c**) ZXY-ZYX axes

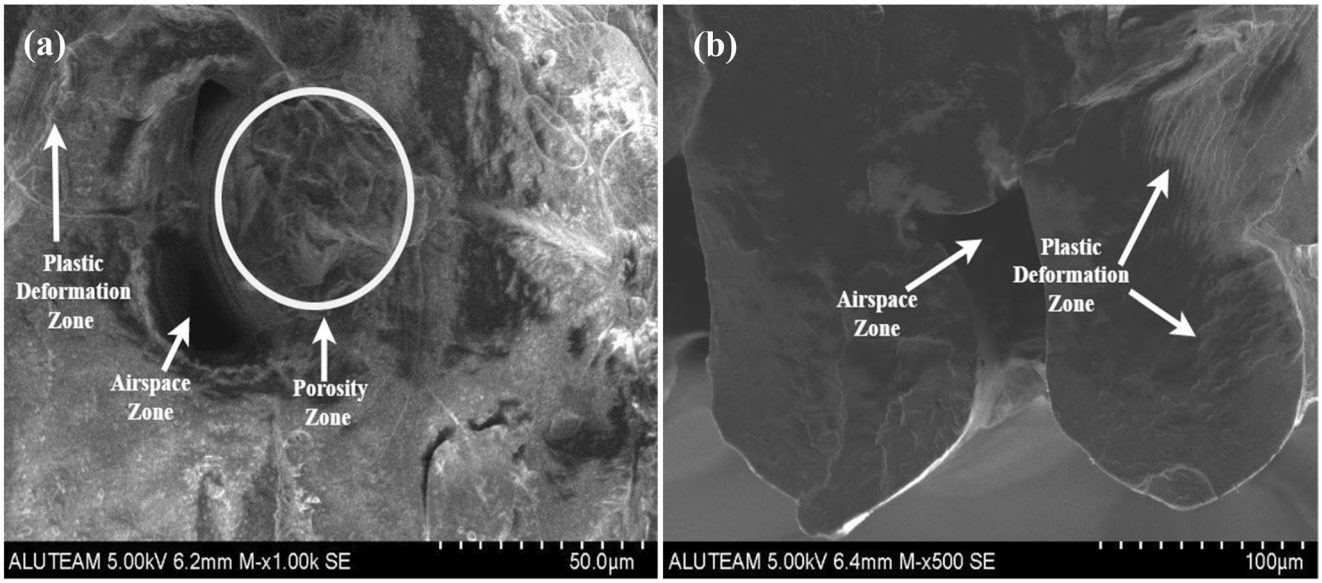

Fig. 10 SEM images of PLA filament according to the XYZ axis: (**a**) X100 and (**b**) X500

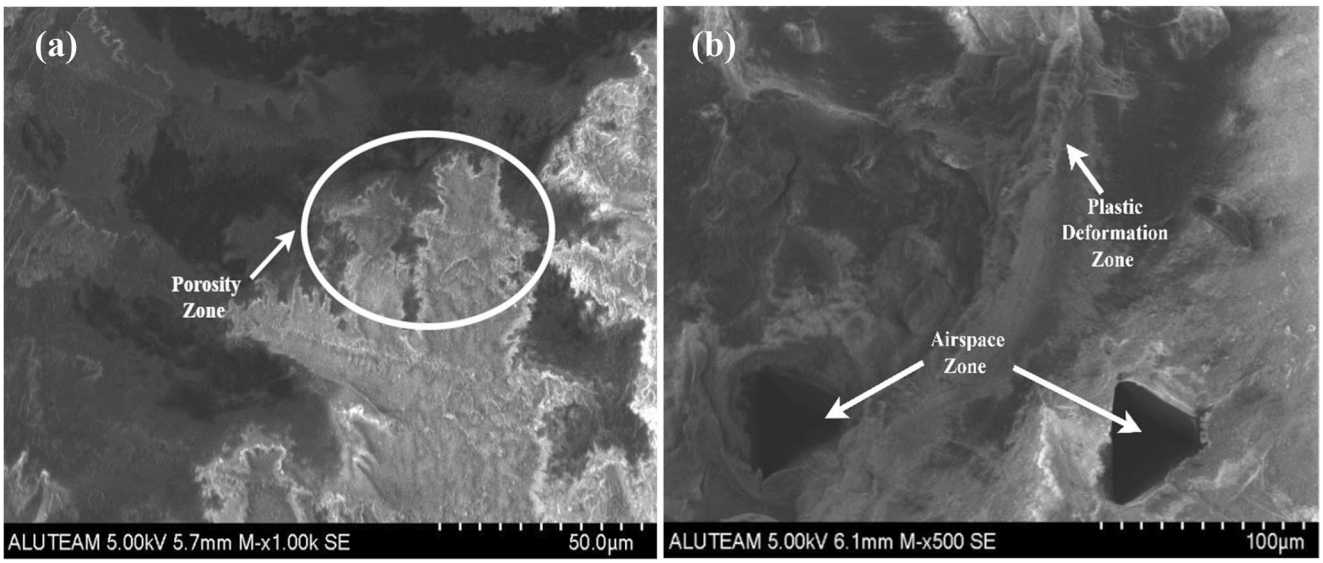

Fig. 11 SEM images of PLA filament according to the XZY axis: (**a**) X100 and (**b**) X500

their mechanical properties. Specimens with lower surface roughness showed higher mechanical properties [52]. In the SEM images, it is seen that there are some voids at different rates at the point where the filament is split into two. It is seen that irregularities and large voids are formed in the images taken from the point where the Re-PLA filament is split into two. The reason for this situation is thought to be due to fractures on the polymer surfaces caused by thermal degradation after the recycling process [51, 55]. During the recycling process, it is thought to undergo degradation due to thermomechanical effects in the blender. As a result, it is also thought to cause a decrease in molecular weight and a decrease in the filament properties of Re-PLA by breaking the chains between monomers [46].

Comparison of different build orientations with PLA and Re-PLA

In this study, when the results obtained from tensile, flexural, and surface roughness tests were combined, it was found that PLA specimens generally exhibited higher tensile strength, while Re-PLA specimens exhibited higher ductility (elongation capacity). In particular, in tensile tests, strength loss was observed in the XYZ and XZY

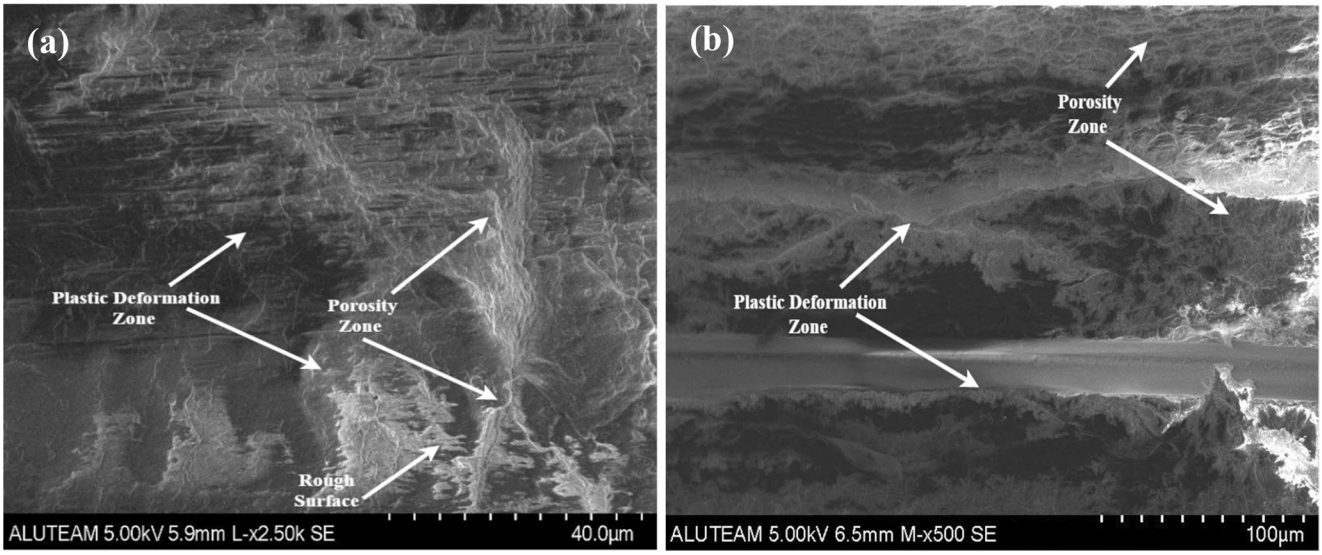

Fig. 12 SEM images of PLA filament according to the ZXY axis: (**a**) X100 and (**b**) X500

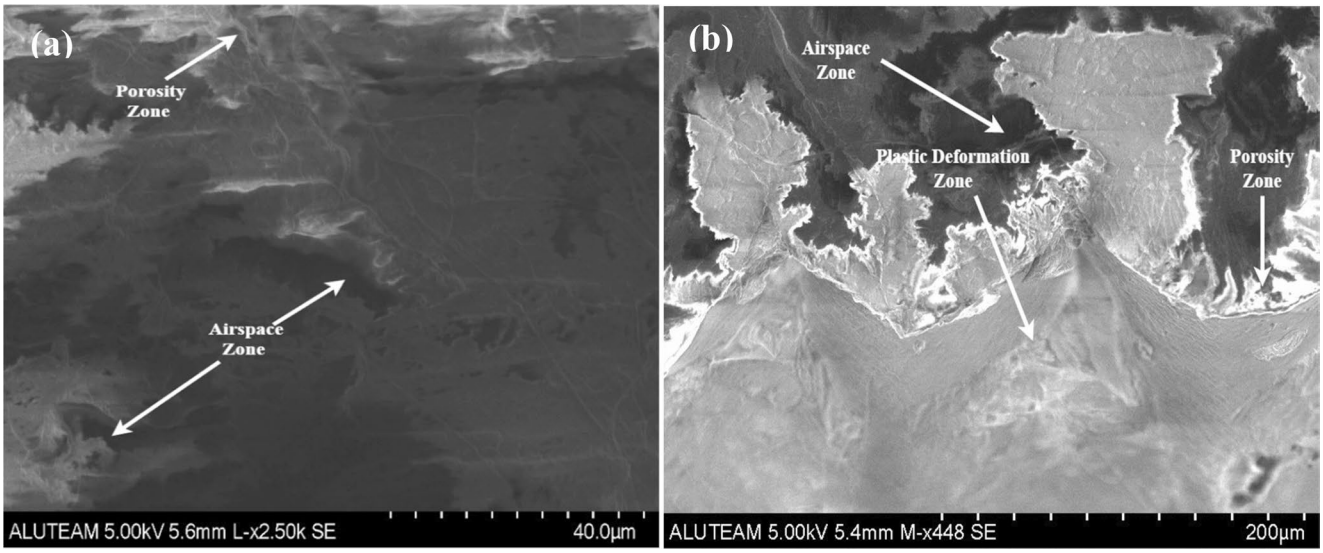

Fig. 13 SEM images of Re-PLA filament according to the XYZ axis: (**a**) X100 and (**b**) X500

directions in PLA, while both materials exhibited similar properties in the YXZ and YZX directions. In bending tests, Re-PLA exhibited significantly higher bending strength in the ZXY-ZYX direction group. Surface roughness measurements indicate that roughness increases in Z-axis prints and can negatively affect mechanical performance.

Literature studies also support these results. Aly et al. (2024) reported in their study using 100% PLA, 100% Re-PLA, and (50% PLA + 50% Re-PLA) filaments that 100% Re-PLA offered 48% higher tensile strength compared to PLA, but performed worse in terms of ductility and toughness [56]. Joshib, (2025) focused on the effect of the printing direction, noting that the porosity ratio decreased in samples printed perpendicular to the Z-axis, thereby enhancing mechanical strength [57].

As a result, both the material type (original-recycled) and the build orientation have a decisive effect on the mechanical and surface properties. In some respects, Re-PLA's performance, which is close to or even superior to that of PLA, reinforces the industrial scalability of recycling. The results of the comparison of the mechanical and surface properties of PLA and Re-PLA specimens for different build orientations are presented in Table 4.

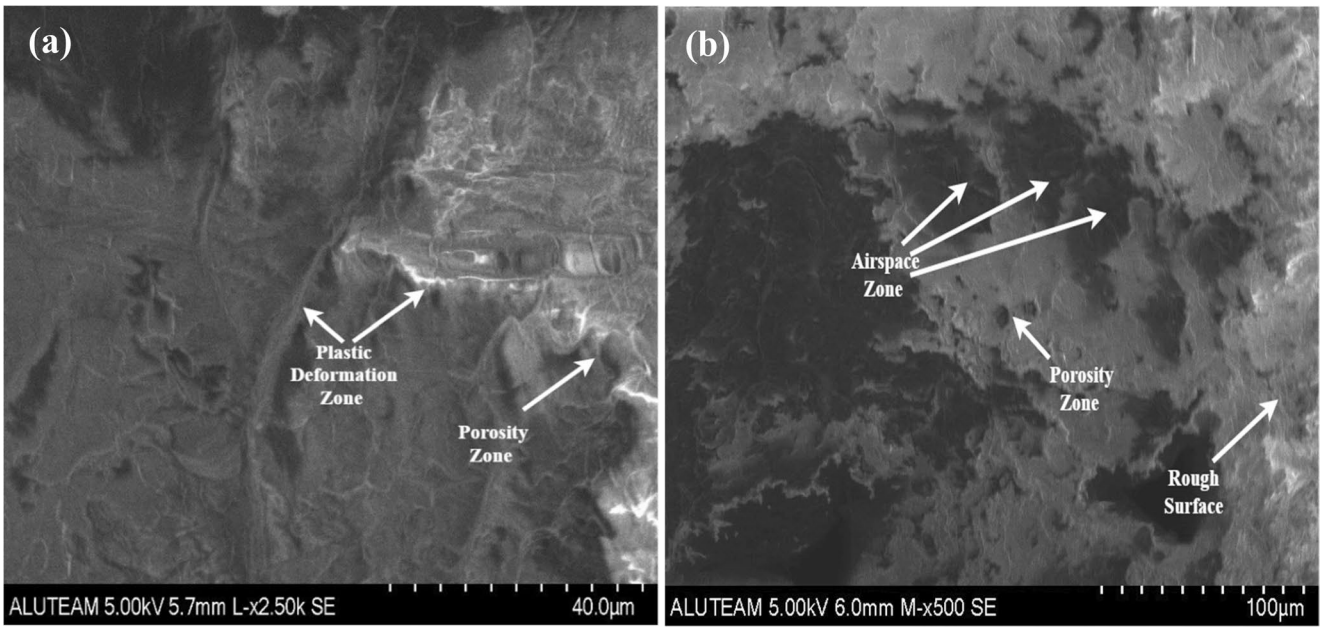

Fig. 14 SEM images of Re-PLA filament according to the XZY axis: (**a**) X100 and (**b**) X500

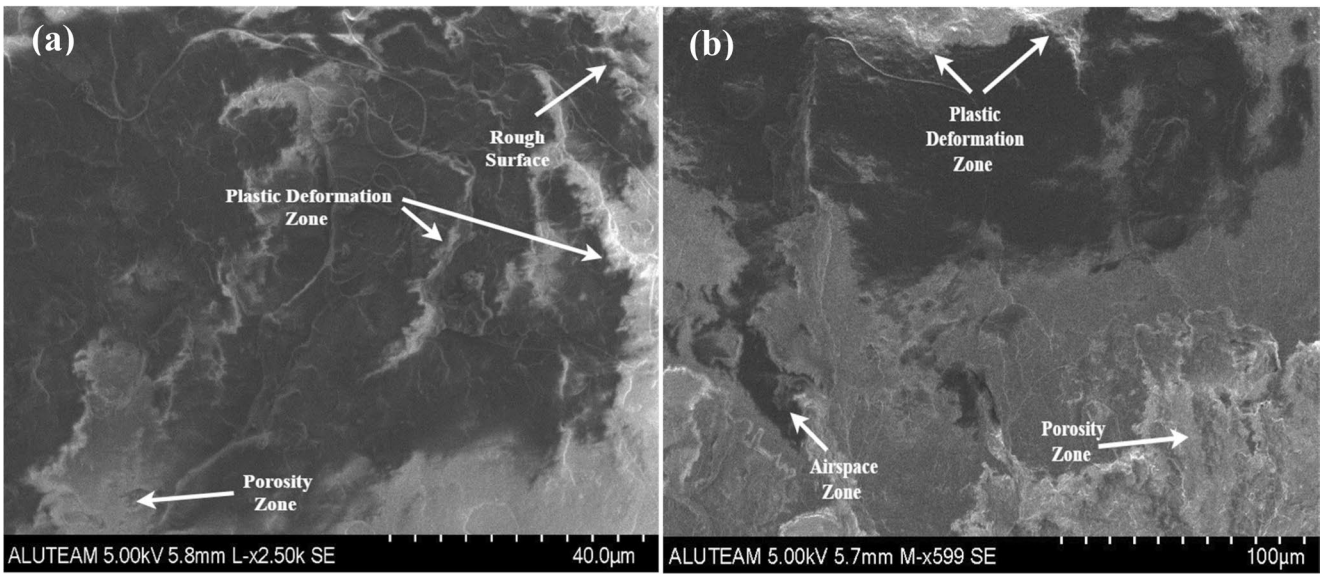

Fig. 15 SEM images of Re-PLA filament according to the ZXY axis: (**a**) X100 and (**b**) X500

Degradation tests results

The degradation behaviors of the specimens were analyzed in PBS medium for 168 min. Since the prepared specimens were intended to be used in the live system, the studies were carried out in PBS buffer. The degradation behaviors of 20%, 40%, 60% PLA, and Re-PLA specimens classified according to their filling ratios in PBS buffer were examined in the wavelength range of 200–800 nm in UV-Vis spectrophotometer devices for 1, 2, 3, 4, 5, 24, 48, 72, 96, 120, 144, and 168 h and no degradation was observed. This is thought to be due to the fact that PLA, which is frequently used in implant materials used in the body, is a hydrophobic polymer and does not dissolve in PBS buffer [58]. No degradation was observed at any time of the degradation study.

Table 4 Comparison of mechanical and surface properties of PLA and Re-PLA specimens for different build orientations

Material	Build Orientation	Tensile Strength	Elongation	Flexural Strength	Surface Roughness	Observation
PLA	XYZ	Medium-low	Medium	Medium	High	Strength reduction along Z-axis, high surface roughness.
	XZY	Medium-low	Medium	Medium	High	Similar Z-axis effect observed.
	YXZ	High	Medium	Medium	Low	More balanced mechanical performance.
	YZX	High	Medium	Medium	Low	Balanced performance.
Re-PLA	XYZ	Medium	High	Medium	High	Higher ductility, lower strength compared to PLA.
	XZY	Medium	High	Medium	High	Similar trend, ductility emphasized.
	YXZ	High	High	Medium	Low	Comparable performance to PLA.
	YZX	High	High	Medium	Low	Comparable or even superior to PLA in some orientations.
	ZXY-ZYX	Medium	High	High	High	Significantly higher flexural strength, good ductility.

Bioactivity test

In recent years, the demand for sustainable materials instead of low-cost and high-strength materials has been triggered globally, which has led researchers to green materials. PLA has emerged as one of the most promising matrix materials for sustainable biopolymers due to its biodegradability, availability, environmental friendliness, antibacterial properties, and favorable mechanical and thermal characteristics [8, 11]. In this study, the antibacterial and cytotoxicity test results of PLA and Re-PLA filaments at different filling ratios are given below within the scope of bioactivity tests.

Antibacterial test results

In the antibacterial activity tests, *E. coli* and *S. aureus* bacteria were tested with 20%, 40%, and 60% of both PLA and Re-PLA specimens in a controlled manner. Figure 16 shows images of (a) *E.coli* and (b) *S. aureus* antibacterial test after 24 h.

Antibacterial activity can vary between gram-negative and gram-positive bacteria because of differences in their cell surface structures [59]. In our tests with *E. coli* and *S. aureus* (Fig. 16a and b), we did not detect any statistically significant antibacterial effect in any of the specimens. The results for PLA and Re-PLA were very similar. That said, we did notice a small, non-significant trend: both PLA and Re-PLA seemed to have slightly lower activity against gram-negative bacteria compared to gram-positive bacteria. This small difference was not strong enough to be considered significant, but it is in line with the known resistance of gram-negative bacteria due to their cell wall characteristics. The fact that the Re-PLA samples, made from recycled waste filaments, performed much like the PLA samples suggests that recycling did not affect their antibacterial performance. PLA is made from lactic acid, mainly the L-lactic acid that comes from biological sources. Lactic acid can exist as meso-, D-, and L-isomers, and differences in the ratio of D- and L-enantiomers in the polymer chain can influence the structure of the polymer [15, 60].

Cytotoxic tests results

According to the measurement results of the obtained biocompatibility experiments, % viability values MTT test results are given in Fig. 17 as a columnar graph. Viability percentages were determined according to the control group using the % cell viability formula. The cell viability of the control group was accepted as 100%.

When the results shown in Fig. 17 are analyzed, PLA 20 exhibited consistently high cell viability, ranging from approximately 98% to 106% over the 1 st, 4th, and 7th days. PLA 40 and PLA 60 showed a moderate decrease in viability over time, with values falling between roughly 75% and 84%. Re-PLA samples maintained cell viability above 70% at all filling ratios and time points, although their values were generally lower than those of the virgin PLA specimens.

In tests performed according to the ISO10993-5 standard; if the cell survival rate is above 70%, the cytotoxicity of the specimen is ignored [61–63]. According to ISO 10993-5, cell adhesion or presence above 70% indicates that the material is non-cytotoxic, while values above 80% indicate good biocompatibility. Specifically, if the plating efficiency is ≥ 70% of the control group, the material shall be considered non-cytotoxic. The results showed that cell viability decreased slightly at all filling ratios when using Re-PLA specimens recycled from waste filaments. It is thought that Re-PLA causes the difference in cell viability due to impurities and sterilization processes in the blending and shredding part of the recycling process. In general, no significant cytotoxic effect on cell viability was detected for all filaments.

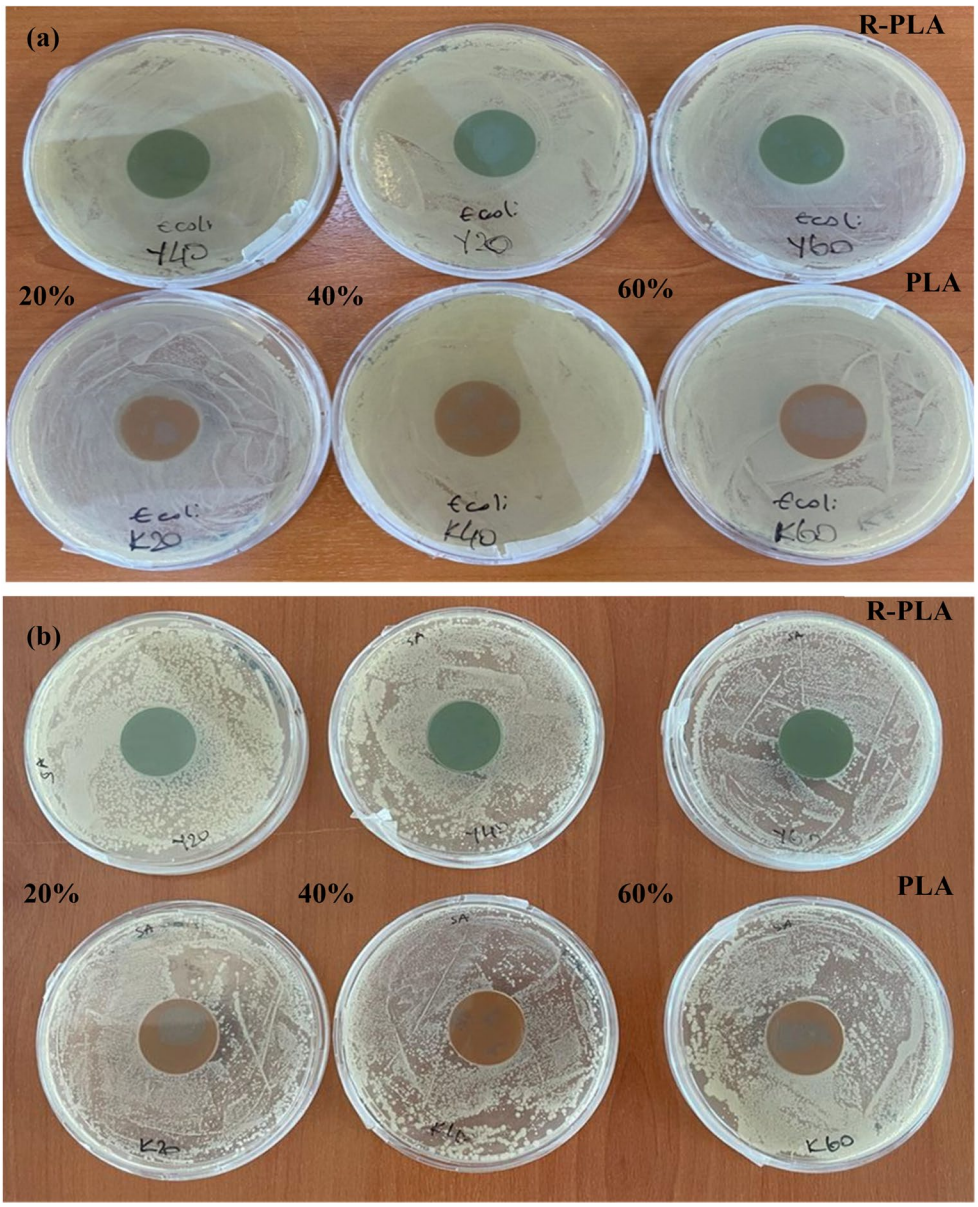

Fig. 16 Antibacterial test results of 24 h (**a**) *E. coli* and (**b**) *S. aureus*

The place of additive manufacturing in PLA sustainability

Environmental, economic, and safety challenges have led packaging scientists and manufacturers to replace petrochemical-based polymers with partially biodegradable ones. The life cycle of PLA, which indicates the steps from PLA production to complete decomposition, is shown in Fig. 18. PLA is a sustainable polymer derived from renewable resources that is fully biodegradable and environmentally friendly. When PLA products reach the end of their life and decompose in the environment, they produce carbon dioxide and water, which are then used in the production of plant products through the process of photosynthesis, as shown in Fig. 18. These agricultural products are again used for PLA production. These important factors ensure the sustainability of PLA polymer [64–66].

Additive manufacturing (AM), also known as 3D printing (3DP), is a manufacturing process that utilizes 3D model data to produce objects by sequentially depositing material layer by layer. Fused deposition modeling involves depositing thermoplastic material layer by layer along specified paths to create 3D objects, making it the most widely used additive manufacturing technology. AM provides an option for the production of periodic lattice structures that are difficult or impossible to produce using traditional methods, as well as the ability to program functional properties on a large scale by adjusting the structure and geometry. Additionally, periodic lattice structures have many additional advantages, such as high stiffness, high bending strength, and high energy absorption at low

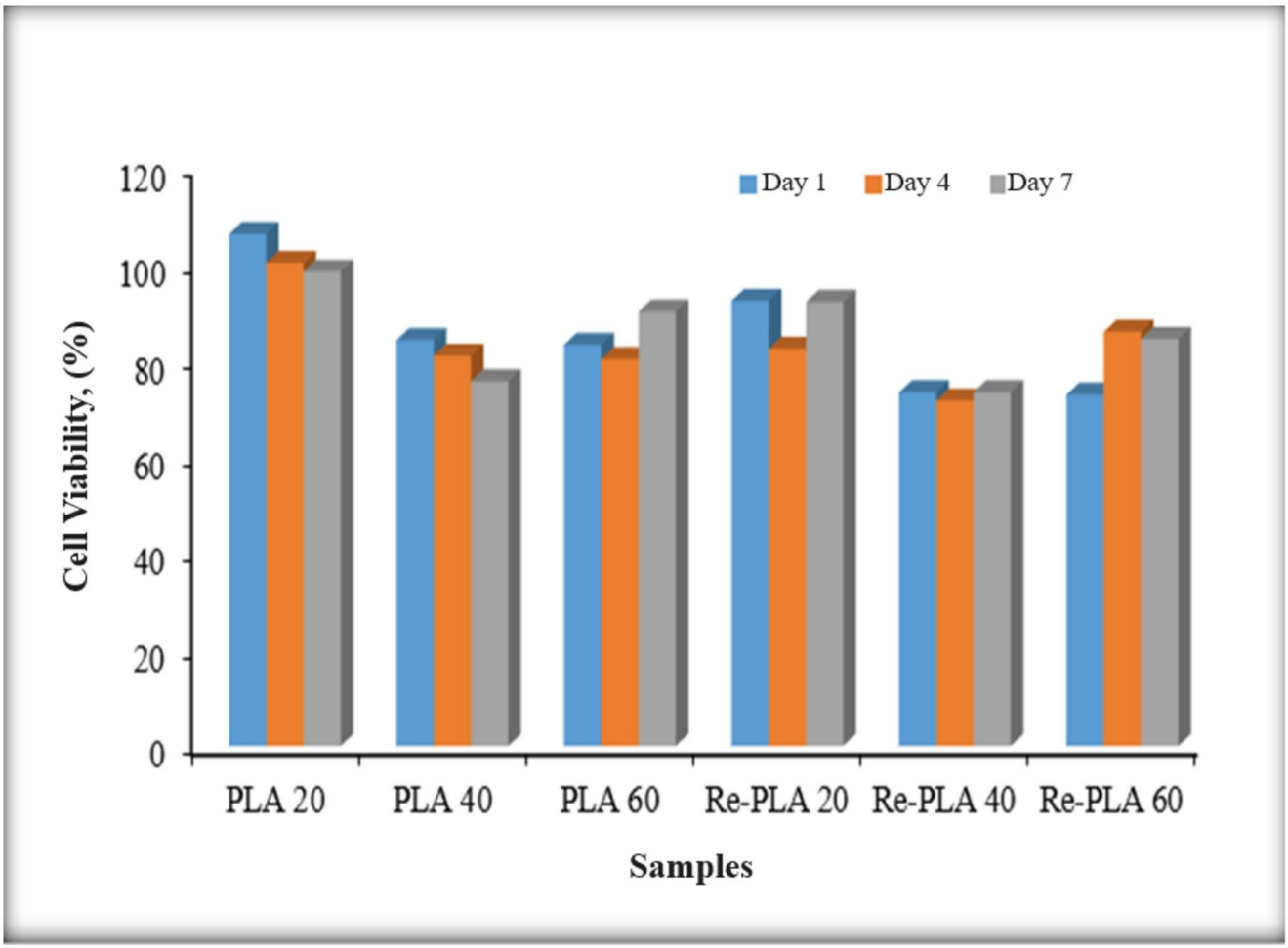

Fig. 17 Comparison of MTT test results

density. Due to the geometric freedom provided by additive manufacturing, a wide variety of lattice materials can be used as cores in sandwich panels, and desired properties can be achieved by changing the cell geometry [64, 67, 68].

With the advantages provided by technological developments, 3D printers have begun to be preferred in the production of both rapid prototyping products and end-user products. AM technologies, provide designers with more flexibility compared to traditional manufacturing methods, as well as many benefits such as low-cost production of small numbers of complex parts, less assembly required for manufactured parts, fewer spare parts in stock, less waste, and advantages in correcting errors in design [67, 68]. There are many different 3D printing methods. Some of the current technologies preferred in additive manufacturing are stereolithography (SLA), fused deposition modeling (FDM), selective laser sintering (SLM), and electron beam melting (EBM). Each of these technologies has its own advantages and disadvantages, and they are specialized for different types of materials [8]. The selection of the method to be applied depends on the purpose of use, material, and desired finish of the part to be manufactured [69]. Due to its low cost, simplicity, and high processing speed, the FDM method is the cheapest and easiest way to develop parts. This rapid prototyping method is preferred in many areas such as automobiles, aviation, medicine, construction, and electricity. PLA is one of the most preferred materials recently because it is obtained from natural resources and is biodegradable. Therefore, revealing the effects of parameters on structural and mechanical properties for specimens manufactured using PLA material is very important for product quality [70].

Conclusion

In this study, PLA and Re-PLA filaments recycled from waste filaments after faulty production were 3D printed in six different orientations, and their mechanical, superficial, degradation, and bioactivity properties were investigated The experimental findings are listed below.

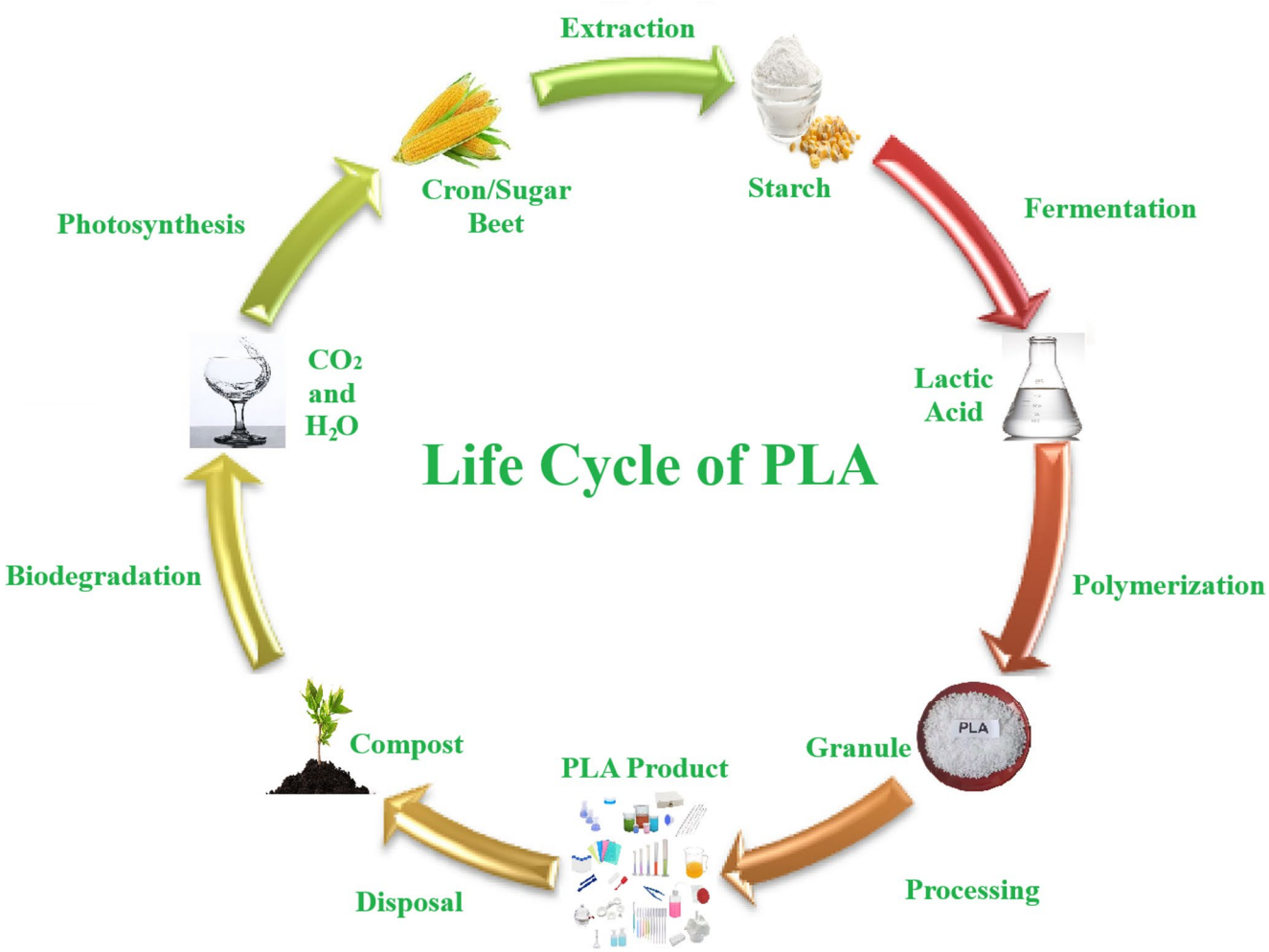

Fig. 18 Life cycle steps of PLA

- The tensile strength of PLA filaments is higher than Re-PLA filaments. While a decrease in the mechanical properties of filaments prepared in XYZ and XZY binary groups was observed. The specimens produced in the ZXY-ZYX binary groups exhibited higher mechanical strength compared to the other groups. It was observed that the specimens produced in other axes showed almost similar properties.
- In both PLA and Re-PLA specimens; Ra values are similar in the test results of XYZ-YXZ, XZY-YZX, and ZXY-ZYX binary groups. Filaments with low surface roughness values showed better mechanical properties than those with high surface roughness. The surface roughness values of PLA and Re-PLA filaments did not change between similar axes in the length and thickness directions but differed in the width direction.
- Additively manufactured Re-PLA filaments become more ductile during the recycling process, and are more subject to shape change than PLA filaments, which are more brittle.
- There was no degradation in PLA and Re-PLA specimens with 20%, 40%, and 60% filling ratios. In terms of biocompatibility, PLA specimens have slightly higher biocompatibility than Re-PLA specimens.
- In line with the results; a positive idea was formed about the supportability of Re-PLA material and as a result, it was understood that the waste of polymer waste can be prevented due to waste PLA material.
- The aim of this study is to bring bio polymers obtained from completely renewable resources such as PLA to the forefront instead of petroleum-based biodegradable polymers in recent years.
- AM/3D printing of recycled polymers is an alternative, distributed, inexpensive method of harmful waste. With the development and adoption of the appropriate techniques, AM can lead to much higher levels of reuse at very low cost and for targeted applications.

Author contributions Conceptualization, Ş.A. and N.B.Ü.; methodology, Ş.A., N.B.Ü. and M.D.; validation, Ş.A. and N.B.Ü.; formal analysis, Ş.A., N.B.Ü. and M.D.; investigation, Ş.A. N.B.Ü. and M.D.; writing-original draft preparation, Ş.A., N.B.Ü. and M.D.; writing-review and editing, Ş.A. and N.B.Ü.; supervision, Ş.A.; project administration, Ş.A. and N.B.Ü.; funding acquisition, Ş.A. and N.B.Ü. All authors have read and agreed to the published version of the manuscript.

Funding Not applicable.

Data availability No data was used for the research described in the article.

Declarations

Conflict of interest The authors declare that they have no known competing financial interests or personal relationships that could have appeared to influence the work reported in this paper.

References

1. 3D Printing: What It Is, How It Works, Examples. In: Investopedia. https://www.investopedia.com/terms/1/3d-printing.asp. Accessed 13 Aug 2025
2. Gibson I, Rosen D, Stucker B, Khorasani M (2021) Additive manufacturing technologies. Springer International Publishing, Cham
3. Attaran M (2017) The rise of 3-D printing: the advantages of additive manufacturing over traditional manufacturing. Bus Horiz 60:677–688
4. Jadhav A, Jadhav VS (2022) A review on 3D printing: an additive manufacturing technology. Mater Today Proc 62:2094–2099
5. Praveena P BA, Lokesh N, A Buradi et al (2022) A comprehensive review of emerging additive manufacturing (3D printing technology): Methods, materials, applications, challenges, trends and future potential. Mater Today: Proc 52:1309–1313
6. Wang Y, Zhou Y, Lin L et al (2020) Overview of 3D additive manufacturing (AM) and corresponding AM composites. Compos Part A Appl Sci Manuf 139:106114
7. Eksi O, Karabeyoglu SS, Cinar K, Muhurcu A (2020) Thermoforming behavior of 3D-printed PLA sheets. Mater Test 62:617–625. https://doi.org/10.3139/120.111522
8. Odera RS, Idumah CI (2023) Novel advancements in additive manufacturing of PLA: a review. Polym Eng Sci 63:3189–3208. https://doi.org/10.1002/pen.26450
9. Subramaniam SR, Samykano M, Selvamani SK et al (2019) 3D printing: overview of PLA progress. In: AIP conference proceedings. AIP Publishing
10. Ilyas RA, Sapuan SM, Harussani MM et al (2021) Polylactic acid (PLA) biocomposite: processing, additive manufacturing and advanced applications. Polymers (Basel) 13:1326
11. Liu Z, Wang Y, Wu B et al (2019) A critical review of fused deposition modeling 3D printing technology in manufacturing polylactic acid parts. Int J Adv Manuf Technol 102:2877–2889. https://doi.org/10.1007/s00170-019-03332-x
12. Tümer EH, Erbil HY (2021) Extrusion-based 3D printing applications of PLA composites: a review. Coatings 11:390
13. Koç HB (2022) Investigation of mechanical properties of products printed with recycled PLAfilament for use in 3D printers. PhD Thesis, Science and Engineering Institue, Marmara University
14. Şahin G (2021) Investigation of mechanical and printing properties of poly(lactic acid) and composite filaments used in 3D printers. MSc. Thesis, Science and Engineering Institue, Trakya University
15. Üner İ, Koçak ED (2012) The area of utilization and electrospinnig applications of poly(lactic acid). Istanbul Commer Univ J Sci 11:79–88
16. Kreiger MA, Mulder ML, Glover AG, Pearce JM (2014) Life cycle analysis of distributed recycling of post-consumer high density polyethylene for 3-D printing filament. J Clean Prod 70:90–96. https://doi.org/10.1016/j.jclepro.2014.02.009
17. polySpectra What Is Build Orientation? Understanding Its Importance in 3D Printing. https://polyspectra.com/what-is-build-orientation/. Accessed 31 Jul 2025
18. Guo H, Xu J, Zhang S, Yi G (2021) Build orientation optimization based on weighted analysis of local surface region curvature. Appl Sci 11:304. https://doi.org/10.3390/app11010304
19. Van Den Eynde M, Van Puyvelde P (2017) 3D printing of Poly(lactic acid). In: Di Lorenzo ML, Androsch R (eds) Industrial applications of Poly(lactic acid). Springer International Publishing, Cham, pp 139–158
20. Torun AR, Dike AS, Yıldız EC et al (2021) Fracture characterization and modeling of gyroid filled 3D printed PLA structures. Mater Test 63:397–401. https://doi.org/10.1515/mt-2020-0068
21. Mamo HB, Adamiak M, Kunwar A (2023) 3D printed biomedical devices and their applications: a review on state-of-the-art technologies, existing challenges, and future perspectives. J Mech Behav Biomed Mater 143:105930. https://doi.org/10.1016/j.jmbbm.2023.105930
22. Myers D, Abdel-Wahab A, Hafeez F et al (2022) Optimisation of the additive manufacturing parameters of polylactic acid (PLA) cellular structures for biomedical applications. J Mech Behav Biomed Mater 136:105447
23. Verbeeten WM, Lorenzo-Bañuelos M (2022) Material extrusion additive manufacturing of poly (lactic acid): influence of infill orientation angle. Addit Manuf 59:103079
24. Ciotti M, Campana G, Mele M (2022) A review of the accuracy of thermoplastic polymeric parts fabricated by additive manufacturing. Rapid Prototyp J 28:358–389
25. Pinho AC, Amaro AM, Piedade AP (2020) 3D printing goes greener: study of the properties of post-consumer recycled polymers for the manufacturing of engineering components. Waste Manag 118:426–434
26. O'Connor HJ, Dickson AN, Dowling DP (2018) Evaluation of the mechanical performance of polymer parts fabricated using a production scale multi jet fusion printing process. Addit Manuf 22:381–387
27. Decuir F, Phelan K, Hollins BC (2016) Mechanical strength of 3-D printed filaments. In: 2016 32nd Southern Biomedical Engineering Conference (SBEC). IEEE, pp 47–48
28. Evlen H, ÖzdemiR MA, Çalişkan A (2019) Effects of filling percentage on mechanical properties of PLA and PET materials. J Polytech 22:1031–1037. https://doi.org/10.2339/politeknik.426413
29. Anderson I (2017) Mechanical properties of specimens 3D printed with virgin and recycled polylactic acid. 3D Print Additive Manuf 4:110–115. https://doi.org/10.1089/3dp.2016.0054
30. Mahir U, Erdoğan YE (2020) Investigation of the effect of using unreinforced and reinforced PLA in production by fused deposition modeling on mechanical properties. J Inst Sci Technol 10:2800–2808
31. Gülcan O (2021) Eklemeli İmalatla Üretilen Kafes Yapıların Mekanik Özellikleri Üzerine Etki Eden Faktörler. Makina Tasarım Ve İmalat Dergisi 19:64–81

32. Maskery I, Aremu AO, Parry L et al (2018) Effective design and simulation of surface-based lattice structures featuring volume fraction and cell type grading. Mater Des 155:220–232
33. Delroisse P, Jacques PJ, Maire E et al (2017) Effect of strut orientation on the microstructure heterogeneities in AlSi10Mg lattices processed by selective laser melting. Scripta Mater 141:32–35
34. Hanon MM, Dobos J, Zsidai L (2021) The influence of 3D printing process parameters on the mechanical performance of PLA polymer and its correlation with hardness. Procedia Manuf 54:244–249
35. Mayén J, Gallegos-Melgar ADC, Pereyra I et al (2022) Descriptive and inferential study of hardness, fatigue life, and crack propagation on PLA 3D-printed parts. Mater Today Commun 32:103948
36. Ji A, Zhang S, Bhagia S et al (2020) 3D printing of biomass-derived composites: application and characterization approaches. RSC Adv 10:21698–21723
37. Wei X, Liu X, Yue C et al (2023) Surface roughness prediction framework for flank milling Ti6Al4V alloy based on CLBAS-BP algorithm. Int J Comput Integr Manuf 36:830–841. https://doi.org/10.1080/0951192X.2022.2145024
38. Bembenek M, Kowalski L, Kosoń-Schab A (2022) Research on the influence of processing parameters on the specific tensile strength of FDM additive manufactured PET-G and PLA materials. Polymers 14:2446
39. Condruz M-R, Paraschiv A, Badea T-A et al (2023) A study on mechanical properties of low-cost thermoplastic-based materials for material extrusion additive manufacturing. Polymers 15:2981
40. Weißmann V, Drescher P, Bader R et al (2017) Comparison of single Ti6Al4V struts made using selective laser melting and electron beam melting subject to part orientation. Metals 7:91
41. Alsalla H, Hao L, Smith C (2016) Fracture toughness and tensile strength of 316L stainless steel cellular lattice structures manufactured using the selective laser melting technique. Mater Sci Engineering: A 669:1–6
42. Kholil A, Syaefuddin EA, Premono A, Nugraha F (2022) The effect of orientation angle and layer thickness on surface roughness of ABS material on FDM. Mater Sci Forum 1057:3–10. https://doi.org/10.4028/p-m37s90
43. Kechagias JD (2024) Surface roughness assessment of ABS and PLA filament 3D printing parts: structural parameters experimentation and semi-empirical modelling. Int J Adv Manuf Technol 134:1935–1946. https://doi.org/10.1007/s00170-024-14232-0
44. Haskul M (2020) Elastic state of functionally graded curved beam on the plane stress state subject to thermal load. Mech Based Des Struct Mach 48:739–754. https://doi.org/10.1080/15397734.2019.1660890
45. Atakok G, Kam M, Koc HB (2022) Tensile, three-point bending and impact strength of 3D printed parts using PLA and recycled PLA filaments: a statistical investigation. J Mater Res Technol 18:1542–1554
46. Tuna B (2021) Investigation of effects of a polymeric chain extender on the properties of recycled poly (butylene terephthalate). BSEU J Sci 8:882–892. https://doi.org/10.35193/bseufbd.974092
47. Mat MC, Ramli FR, Alkahari MR et al (2020) Influence of layer thickness and infill design on the surface roughness of PLA, PETG and metal copper materials. Proc Mech Eng Res Day 7:64–66
48. Torrado AR, Shemelya CM, English JD et al (2015) Characterizing the effect of additives to ABS on the mechanical property anisotropy of specimens fabricated by material extrusion 3d printing. Addit Manuf 6:16–29
49. Rankouhi B, Javadpour S, Delfanian F, Letcher T (2016) Failure analysis and mechanical characterization of 3D printed ABS with respect to layer thickness and orientation. J Fail Anal Preven 16:467–481. https://doi.org/10.1007/s11668-016-0113-2
50. Tekinalp HL, Kunc V, Velez-Garcia GM et al (2014) Highly oriented carbon fiber–polymer composites via additive manufacturing. Compos Sci Technol 105:144–150
51. Sanchez FAC, Boudaoud H, Hoppe S, Camargo M (2017) Polymer recycling in an open-source additive manufacturing context: mechanical issues. Addit Manuf 17:87–105
52. Chawla K, Singh R, Singh J (2022) On recyclability of thermoplastic ABS polymer as fused filament for FDM technique of additive manufacturing. World J Eng 19:352–360
53. Letcher T, Waytashek M (2014) Material property testing of 3D-printed specimen in PLA on an entry-level 3D printer. In: Metghalchi H (ed) ASME international mechanical engineering congress and exposition. American society of mechanical engineers. V02AT02A014
54. Callister WD, Rethwisch DG (1999) Materials science and engineering: an introduction. Wiley, New York
55. Kamer MS, TemiZ Ş, Yaykaşli DH et al (2022) Comparison of mechanical properties of tensile test specimens produced with ABS and PLA material at different printing speeds in 3D printer. J Fac Eng Archit Gazi Univ 37:1197–1212. https://doi.org/10.17341/gazimmfd.961981
56. Aly R, Olalere O, Ryder A et al (2024) Mechanical property characterization of virgin and recycled PLA blends in single-screw filament extrusion for 3D printing. Polymers 16:3569
57. Joshib R (2025) Investigation on tensile and compression properties of 3D printed PLA material for various infill percentage. Indian Sci J Res Eng Manage 9:1–9. https://doi.org/10.55041/ijsrem41134
58. Hajilou N, Mostafayi SS, Yarin AL, Shokuhfar T (2024) A comparative review on biodegradation of poly (lactic acid) in soil, compost, water, and wastewater environments: incorporating mathematical modeling perspectives. AppliedChem 5:1
59. Gürler N, Yazdıç FC (2023) Physical and antibacterial activities of 3-Aptms reinforced chitosan-polyvinyl alcohol blend films. Kahramanmaras Sutcu Imam Univ J Eng Sci 26:154–165
60. Senatov FS, Niaza KV, Zadorozhnyy MY et al (2016) Mechanical properties and shape memory effect of 3D-printed PLA-based porous scaffolds. J Mech Behav Biomed Mater 57:139–148
61. Altınsoy Ş, Erkan S, Üllen NB et al (2024) Evaluation of surface properties of modified Ti6Al4V alloy with copper nanoparticles organic nanostructure for biomedical applications: dependency on anticorrosive, antibacterial, and biocompatibility. Corros Rev. https://doi.org/10.1515/corrrev-2023-0148
62. Altınsoy Ş, Kızılbey K, İlim HB (2024) Green synthesis of Ag and Cu nanoparticles using *E. telmateia* Ehrh extract: coating, characterization, and bioactivity on PEEK polymer substrates. Materials 17:5501
63. Wallin RF, Arscott EF (1998) A practical guide to ISO 10993-5: cytotoxicity. Med Device Diagn Ind 20:96–98
64. Raddadi N, Fava F (2019) Biodegradation of oil-based plastics in the environment: existing knowledge and needs of research and innovation. Sci Total Environ 679:148–158
65. Scaffaro R, Maio A, Gulino EF, Megna B (2019) Structure-property relationship of PLA-Opuntia ficus indica biocomposites. Compos Part B: Eng 167:199–206
66. Trivedi AK, Gupta MK, Singh H (2023) PLA based biocomposites for sustainable products: a review. Adv Ind Eng Polym Res 6:382–395

67. Javaid M, Haleem A, Singh RP et al (2021) Role of additive manufacturing applications towards environmental sustainability. Adv Ind Eng Polym Res 4:312–322
68. Sanchez-Rexach E, Johnston TG, Jehanno C et al (2020) Sustainable materials and chemical processes for additive manufacturing. Chem Mater 32:7105–7119. https://doi.org/10.1021/acs.chemmater.0c02008
69. Kafle A, Luis E, Silwal R et al (2021) 3D/4D printing of polymers: fused deposition modelling (FDM), selective laser sintering (SLS), and stereolithography (SLA). Polymers 13:3101
70. Rajaguru K, Karthikeyan T, Vijayan V (2020) Additive manufacturing–state of art. Mater Today Proc 21:628–633

Publisher's note Springer Nature remains neutral with regard to jurisdictional claims in published maps and institutional affiliations.

Springer Nature or its licensor (e.g. a society or other partner) holds exclusive rights to this article under a publishing agreement with the author(s) or other rightsholder(s); author self-archiving of the accepted manuscript version of this article is solely governed by the terms of such publishing agreement and applicable law.